MINISTÉRIO DA EDUCAÇÃO
UNIVERSIDADE FEDERAL DO RIO GRANDE DO SUL
PROGRAMA DE PÓS-GRADUAÇÃO EM ENGENHARIA MECÂNICA

SIMULATION OF POWER PLANTS STEAM GENERATORS AND COOLING TOWERS WITH ARTIFICIAL NEURAL NETWORK

Helena Haas Reichert

Dissertação para obtenção do Título de
Mestre em Engenharia

Porto Alegre, Maio de 2019

SIMULATION OF POWER PLANTS STEAM GENERATORS AND COOLING TOWERS WITH ARTIFICIAL NEURAL NETWORK

por

Helena Haas Reichert
Engenheira de Energia

Dissertação submetida ao Corpo Docente do Programa de Pós-Graduação em Engenharia Mecânica, PROMEC, da Escola de Engenharia da Universidade Federal do Rio Grande do Sul, como parte dos requisitos necessários para a obtenção do Título de

Mestre em Engenharia

Área de Concentração: Fenômenos de transporte

Orientador: Prof. Dr. Paulo Smith Schneider
Co-orientador: Prof. Dr. João Gari da Silva Fonseca Junior

Aprovada por:

Prof. Dr. Antônio José da Silva Neto..... UDT/LEMec / UERJ

Prof. Dr. Marcelo Farenzena.....DEQUI / UFRGS

Prof. Dr. Letícia Jenisch Rodrigues.....PROMEC/UFRGS

Prof. Dr. Fernando Marcelo Pereira
Coordenador do PROMEC

Porto Alegre, 30 de Maio de 2019

AGRADECIMENTOS

Agradeço a minha família pelo apoio, confiança e incentivo. Em especial, agradeço aos meus pais, Andreana e Geraldo, pelo carinho e exemplo. À minha irmã pelo companheirismo. E ao Lucas por ter me acompanhado e incentivado em todos os momentos.

Agradeço também aos meus colegas e amigos de mestrado. Agradeço a equipe de pesquisa do projeto SMART-PÉCEM pelo incentivo no desenvolvimento desse trabalho.

A todos os professores que fizeram parte da minha formação, especialmente aos professores Paulo Smith Schneider e João Gari da Silva Fonseca Junior, pela orientação, apoio e confiança.

Agradeço a Energia de Portugal (EDP) pelo suporte financeiro que possibilitou o desenvolvimento do projeto de pesquisa e desenvolvimento, SMART-PÉCEM. Ainda, agradeço a equipe da EDP pela contribuição no desenvolvimento deste trabalho.

Por fim, agradeço a Coordenação de Aperfeiçoamento de Pessoal de Nível Superior (CAPES) pelo suporte financeiro.

RESUMO

A modelagem da operação de equipamentos é uma opção metodológica importante para a melhoria da eficiência de usinas geradoras de energia. Uma dessas metodologias é a rede neural artificial (RNA), que vem ganhando espaço devido à sua capacidade de modelar problemas complexos com base em comportamentos registrados de sistemas reais. O objetivo do presente estudo é desenvolver modelos de RNA capazes de reproduzir o funcionamento do gerador de vapor e da torre úmida de arrefecimento da planta termoelétrica a carvão de PECÉM, no estado do Ceará, Brasil. O modelo de RNA para o gerador de vapor superaquecido a carvão estima a vazão mássica de vapor com base em registros de um ano de operação da Usina. A configuração das RNAs é obtida após uma série de testes com o objetivo de reduzir o erro de predição através do erro absoluto médio (EAM) em diferentes patamares de operação, obtendo-se um MAE de 1,28% para o conjunto total de dados de operação, 8,11% para a faixa de operação de 240 MW e 10,82% para a faixa de operação de 360 MW. O desempenho das redes é comparado ao de modelos de regressão linear múltipla aplicados ao mesmo conjunto de dados, para os quais se têm valores de MAE de 2,05%, 9,47% e 15,76%. Esses resultados mostram a capacidade da RNA de estimar a produção de vapor com erro abaixo daqueles de modelos de regressão. O modelo de RNA é desenvolvido para um dos conjuntos de torres úmidas de resfriamento ligado ao sistema de condensação de uma das plantas do sitio de geração. Essa planta é referenciada como de melhor desempenho e o modelo RNA gerado é aplicado aos dados de operação do segundo conjunto de torres, ajudando na identificação de possíveis desvios ou problemas de desempenho. Ferramentas estatísticas são usadas para avaliar os dois conjuntos de dados referentes as torres de cada usina e identificar correlações de parâmetros. Os modelos de RNA com melhor desempenho são obtidos com um coeficiente máximo de correlação R^2 de 0,9956 para a taxa de calor rejeitada e 0,8699 para a taxa de vazão mássica de água de reposição para o conjunto de dados de referência. O coeficiente R^2 encontrado para o segundo conjunto de torres é de 0,748 para a taxa de calor rejeitada e 0,905 para a vazão mássica de água de reposição. Esse resultado ajuda a identificar alguns comportamentos não padronizados da torre. Uma nova simulação sem os pontos de fora da curva (outlier) exibiu valores de R^2 de 0,98 e 0,99, respectivamente.

Palavras-chave: Redes neurais artificiais; Gerador a vapor superaquecido; Torre úmida de arrefecimento; Modelagem da operação de usinas termelétricas a carvão.

ABSTRACT

The modeling of equipment operation is an important methodological option for improving the efficiency of power plants. One of these methodologies is the artificial neural network (ANN), which is gaining space due to its ability to model complex problems based on acquired data from real systems. The objective of the present study is to develop ANN models capable of reproducing the operation of the steam generator and the wet cooling tower of the PECÉM coal-fired power plant in the state of Ceara, Brazil. The ANN model for the coal superheated steam generator estimates the steam mass flow rate based on year-long records of operation. ANN configuration is obtained after a series of tests with the objective of reducing the ANN mean absolute error (MAE) in different levels of operation, obtaining an MAE of 1,28% for the total set of data of operation, 8.11% for the 240 MW operating range and 10.82% for the 360 MW operating range. The network performance is compared to that of multiple linear regression models applied to the same data set, with MAE values of 2.05%, 9.47% and 15.76%. These results show the ability of ANN to estimate the production of vapor with errors below those of regression models. The ANN model is developed for one set of wet cooling towers connected to the condensation system. This plant is referred to present the best performance and the generated ANN model is applied to the operation data of the second plant, helping to identify possible deviations or performance problems. Statistical tools are used to evaluate the two cooling towers and to identify parameter correlations. The best performing ANN models are obtained with a R^2 correlation coefficient of 0.9956 for the rejected heat rate and 0.8699 for the makeup water mass flow rate for the reference data set. The coefficient R^2 found for the second set of towers is 0.748 for the rejected heat rate and 0.905 for the makeup water mass flow rate. This result helps to identify some non-standard behavior of the tower. A new simulation without the outlier points exhibited R^2 values of 0.98 and 0.99, respectively.

Keywords: Artificial neural networks; Super-heated steam generator; Wet cooling tower; Coal-fired power plant modeling.

INDEX

1	**INTRODUCTION .....**	**1**
1.1	Thesis Objectives…….……..	4
1.2	Thesis Outline……	4
2	**A REVIEW ON THE APPLICATION OF ANN TECHNIQUES FOR POWER PLANT MODELING…….....**	**5**
2.1	Introduction……	5
2.2	Artificial neural networks……...	5
2.2.1	History……...	5
2.2.2	Brief description…….	6
2.2.3	Learning process……	8
2.2.4	ANNs architecture……..	9
2.2.5	Multiple layer perceptron……...	10
2.2.5.1	Activation function……	11
2.2.5.2	Backpropagation……..	11
2.3	ANNs applied to steam generators……...……...……	12
2.3.1	ANNs applied to steam generators bibliometric…….	19
2.4	ANNs applied to wet cooling towers…….....……	20
2.4.1	ANNs applied to cooling towers bibliometric…….	22
2.5	Dataset……....……....	23
2.6	Conclusions…….	23
3	**STEAM FLOW ESTIMATION WITH ARTIFICIAL NEURAL NETWORK BASED ON POWER PLANT OPERATIONAL DATA.....**	24
3.1	Introduction…….	24
3.2	Problem description…….	25
3.3	Methodology……...	26
3.4	Results and discussion…….	33
3.4.1	Linear Multiple Regression…….	33
3.4.2	Artificial Neural Network……	36
3.5	Conclusions…….	41
4	**PERFORMANCE ESTIMATION OF A COOLING TOWER USING AN**	43

	ANN MODEL…….....	
4.1	Introduction…….	43
4.2	Problem description……	45
4.3	Methodology……...	47
4.3.1	Statistical analysis……...	47
4.3.2	Artificial neural network……	52
4.4	Results and discussion…….	53
4.5	Conclusion……	56
5	**CONCLUSIONS.....**	58
5.1	Future works……	59
6	**PUBLICATIONS……**	60
	BIBLIOGRAPHY.....	61

LIST OF FIGURES

Figure 1.1	World CO_2 emission from fuel combustion [International Energy Agency, 2017] ……..….....	1
Figure 1.2	Brazilian energy matrix [ANEEL, 2019] ……..……	2
Figure 2.1	Artificial Neuron proposed by McCulloch and Pitts [Adapted from Haykin, 2009]	7
Figure 2.2	Diagram of the supervised learning method [Adapted from Haykin, 2001].…….....	8
Figure 2.3	Perceptron Architecture of Multiple Layers.....	10
Figure 2.4	Schematic representation of a steam generator.....	12
Figure 2.5	Bibliometrics: Publications years of steam generator studies……	19
Figure 2.6	Bibliometrics of (a) Steam generator articles dataset; (b) Steam generator articles models comparison……	20
Figure 2.7	Direct contact or open evaporative cooling tower schematic view [Adapted from ASHRAE, 2016]…...…….	20
Figure 3.1	PECEM Superheated Steam Generator SSG.....	25
Figure 3.2	Block 1- Data processing.....	27
Figure 3.3	Steam generator correlation matrix	29
Figure 3.4	Methodology scheme for Linear multiple regression (Block 2), ANN (Block 3) and Conclusions (Block 4)	30
Figure 3.5	PECEM electric power output levels as a function of the vapor condensation pressure …….....	31
Figure 3.6	ANN architecture developed for steam flow estimation.....	33
Figure 3.7	Regression evaluation for training data size.....	34
Figure 3.8	Regression evaluation for number of inputs.....	34
Figure 3.9	ANN evaluation for each set configuration as a function of the training data size …….....	36
Figure 3.10	ANN evaluation for number of inputs.....	37
Figure 3.11	Calculated errors RMSE and MAE for several ANN with data from plant 240 MW power output.....	38
Figure 3.12	Calculated errors RMSE and MAE for several ANN with data from plant 360 MW power output.....	38

Figure 3.13	ANN and regression RMSE for selected models…….……	40
Figure 4.1	Counterflow cooling tower operation [ASHRAE, 2016].....	44
Figure 4.2	(a) PECEM plant cooling system compost by the consortium, heat exchanger, pump and cooling tower assembly. (b) Schematic representation of a cooling tower	45
Figure 4.3	Matrix correlation for GP1.....	48
Figure 4.4	Matrix correlation for GP2.....	49
Figure 4.5	Data plotting with the behavior of the rejected heat $\dot{Q_{rej}}$ in respect to the measured parameters vapor backpressure BP, input and output water temperature T_{in} and T_{out} and power generation P for GP1 (a to d) and GP2 (e to h)	50
Figure 4.6	Data plotting with the behavior of the makeup water mass flow rate $\dot{m_{w,r}}$ in respect to the measured parameters vapor backpressure BP, input and output water temperature T_{in} and T_{out} and power generation P for GP1 (a to d) and GP2 (e to h)	51
Figure 4.7	ANN inputs (a) heat rejected and (b) makeup water mass flow.....	53
Figure 4.8	Estimated vs. calculated results for the normalized makeup water mass flow with ANN_4_4_4_1 (Table 4.4) for GP2 dataset.....	54
Figure 4.9	Estimated *vs.* calculated results for the normalized heat rejected rate with ANN_4_4_4_1(Table 4.4) for GP2 dataset.....	54
Figure 4.10	Estimated *vs.* calculated results for the rejected heat rate with ANN_4_4_4_1 for the modified GP2 dataset.....	55
Figure 4.11	Estimated *vs.* calculated results for the makeup water flow mass rate with ANN_4_4_4_1 for the modified GP2 dataset.....	55

LIST OF TABLES

Table 2.1	Review of papers using ANN for problems involving steam generators…….....	17
Table 3.1	SSG maximum and minimum values	26
Table 3.2	Dataset Pearson correlation index for the SSG parameters from Table 3.1 for the plant yearlong dataset …….....	28
Table 3.3	Regression evaluation for operation stages.....	35
Table 3.4	Set configurations with particular ranges for training data size.....	36
Table 3.5	Steam mass flow rate ANN architectures performance with the complete dataset……....	37
Table 3.6	Steam mass flow rate ANN architectures errors for the transition stage …….....	39
Table 3.7	ANN evaluation for operation stages.....	40
Table 4.1	Operating range of the two towers parameters.....	46
Table 4.2	Dataset Pearson correlation index for GP1.....	47
Table 4.3	Dataset Pearson correlation index for GP2.....	48
Table 4.4	ANN configuration analysis GP1.....	54

LIST OF ABBREVIATIONS

ANN	Artificial Neural Network
BProp	Back-Propagation
CHP	Combined Heat and Power
FFBP	Feed-Forward Back-Propagation
FFNN	Feed-Forward Neural Network
GA	Genetic Algorithm
GCV	Gross Calorific Value
GP1	Generation Plant 1
GP2	Generation Plant 2
HHV	Higher Heating Value
LM	Levenberg-Marquardt
MAE	Mean Absolute Error
MLP	Multi-Layer Perceptron
MLPNN	Multi-Layer Perceptron Neural Network
NARX	Nonlinear Autoregressive Exogenous
NARXNN	Nonlinear Autoregressive Exogenous Neural Network
nntool	Neural network tool
RMSE	Root Mean Squared Error
RP	Radial Propagation
SSG	Superheated Steam Generators
trainlm	Training Levenberg-Marquardt
US	United States

LIST OF SYMBOLS

Latin Symbols

b	Bias, -
BP	Vapor Back Pressure, mbar
CO_2	Carbon dioxide, -
cp_w	Water specific heat, J/(kg K)
$\dot{m_{air,o}}$	Output air mass flow rate, kg/s
$\dot{m_{air,1}}$	Primary air flow, kg/s
$\dot{m_{air,2}}$	Secondary air flow, kg/s
$\dot{m}_c$	Coal mass flow rate, t/h
$\dot{m_{OFA}}$	Over fire air flow, kg/s
$\dot{m}_s$	Steam mass flow rate, t/h
$\dot{m_{water}}$	Tower water flow, m³/h
$\dot{m_{w,i}}$	Tower water flow in, m³/h
$\dot{m_{w,o}}$	Tower water flow out, m³/h
$\dot{m_{w,r}}$	Makeup water mass flow rate, m³/h
n	Number of data points, -
NO_x	Nitrogen oxides, -
P	Power plant, MW
P_s	Steam pressure, MPa
O_2	Oxygen level, %
$\dot{q}_a$	Air heat rejected
$\dot{Q_{rej}}$	Heat rejected flow, MW
$\dot{q}_w$	Water heat rejected
R^2	Coefficient of correlation, -
T	Temperature, ºC
T_{db}	Dry bulb temperature, ºC
T_{in}	Tower water input temperature, ºC
T_{out}	Tower water output temperature, ºC
T_w	Water temperature, ºC
T_{wb}	Wet bulb temperature, ºC

v_k	Neuron, -
w_{kj}	Synaptic weight, -
x	Input, -
X_{est}	Estimated value, -
X_{obs}	Observed value, -
Y	Output signal ,-

Greek Symbols

a	Slope, -
ΔT_w	Temperature Difference in Water Circuit, ºC
$i_{l,v}$	Latent heat of vaporization, J/kg
ρ	Density, kg/m³
φ	Activation function, -

Subscripts

ar	air
c	Coal
est	Estimated
obs	Observed
OFA	Over Fire Air
r	Reposition
rej	Rejected
s	Steam
w	Water

1 INTRODUTION

Several studies related to climate change pointed out the impact of global warming on many countries economies and social development [European Environment Agency, 2017]. Fuel consumption is claimed to produce a large amount of CO_2 emissions to the atmosphere, as presented in Figure 1.1

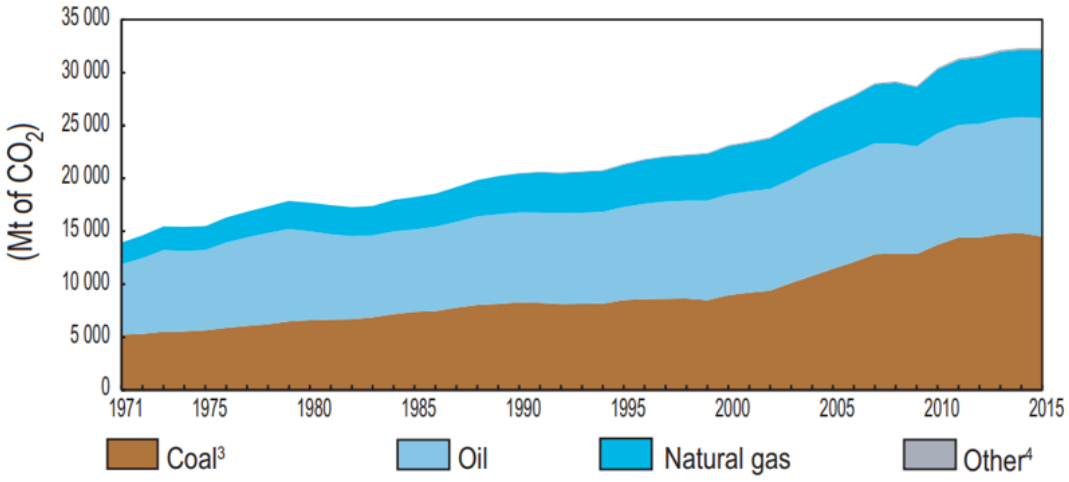

Figure 1.1 – World CO_2 emission from fuel combustion [International Energy Agency, 2017].

Among all fuels, coal combustion represents an important share of emitted greenhouse gases, with 14,535 Mt CO_2 in 2015, burned in power plants. Nevertheless, electricity production with coal will remain necessary as a base load option or a complement backup due to intermittent sources [Starkloff et al., 2015].

Fossil fuels represent 24.5% of the Brazilian electric power generation, with 40.42 MW of installed capacity [ANEEL, 2019]. These numbers show that thermal plants security the Brazilian energy matrix, besides the role of hydroelectricity, as shown in Figure 1.2.

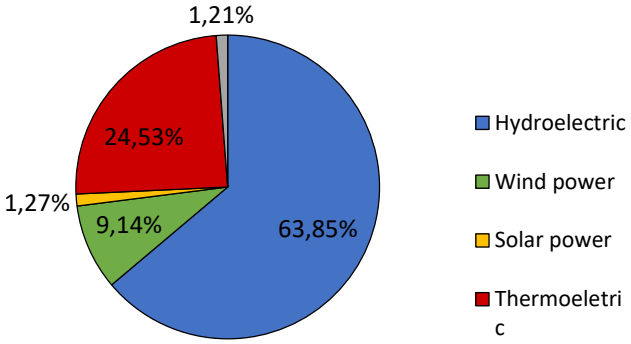

Figure 1.2 – Brazilian energy matrix [ANEEL, 2019].

Several studies focus on enhancing coal-fired plant efficiency as they are necessary to guarantee the stability of the electric grid. These plants are usually designed to operate at full load for long periods, but new market restrictions are continuously reducing operation setups due to the contribution of intermittent energy sources, such as hydroelectric, on the grid. As a result, power plant operators are forced to develop novel and efficient solutions to operate under these circumstances [Starkloff et al., 2015].

Modeling complexity of coal-fired power plants is a well-known matter, highlighted in several studies. Different methodologies and models are applied to simulate the power plant systems or equipment. Studies related to this subject result in the improvement of the process efficiency.

Zhang et al., 2006, modeled a coal-fired power plant based on mass and energy balances for different operating conditions to perform a thermo-economic analysis, with relative errors less than 2%. However, that particular case study focused on the plant exergy cost analysis.

Fan et al., 2017, developed a dynamic mathematical model based on mass and energy balances associated with a genetic algorithm to achieve plant optimization. Their model could simulate and test control algorithms with 50% more accuracy than the reference model used in that study. Although the model good accordance, it was not meant to be used without a great deal of development effort to be adapted to new situations.

Starkloff et al., 2015, presented an investigation on the operational flexibility of a coal-fired power plant to market scenarios. Their model was able to simulate plant operation within a wide load range (27.5% to 100%) with high accuracy, validated with power plant real data. However, the model complexity turned its application for different cases hard to be implemented.

The model developed by Hübel et al., 2017, investigated the optimization potential related to power plant control systems, such as costs and environmental impacts. That model focused on the start-up operation stage, and could not be used for steady state regime. It aimed to identify restrictions for faster start-ups, less fuel consumption and emissions with controlled thermal and mechanical stress.

Liu et al., 2015, developed a low complexity model to perform control strategies of a given power generation system based on fundamental physic laws. The maximum relative error of that model was 3%, which is a good result for a simple control model.

Among the options for modeling high complexity systems, the use of Artificial Neural Networks ANNs showed to be an attractive approach. They have been used in recent years due to their multiple advantages in prediction, classification and forecasting applications, as they display high potential to describe complex problems. Furthermore, ANN models are compared to other techniques to evaluate model performance with adequate accuracy when compared to other well-stablished methodologies.

Bekat et al., 2012, developed an ANN model to predict the ratio of produced bottom ash to burned coal in a coal-fired power plant. The developed model presented a coefficient of correlation R^2 of 0.984, which can be considered as a good achievement for the estimating such a complex parameter. Furthermore, the model was able to evaluate the most effective parameter associated to the prediction of that ratio.

Tunckaya and Koklukaya, 2015a, pointed out several limitations related to power plant operation, such as cost of energy production, optimization problems related to production and emission levels. One power plant was modeled with ANN and multiple linear regression, but the first one presented the best performance with R^2 of 0.992 and RMSE of 0.1642.

Tunckaya and Koklukaya, 2015b, highlighted that global regulation imposes several improvements on existing coal-fired power plants through the implementation of emission reduction systems and efficiency improvements, but with high investment impacts on plants. A comparative study on the modeling of coal plants was carried out and the emission estimation was achieved with an ANN model, with R^2 of 0.949 and RMSE of 0.819, which were approximately 85% and 95% lower than the RMSE values of the concurrent models.

The reported studies for power plant simulation expressed the ability of ANN algorithms to estimate power plant parameters, pointed out that they are appropriate to describe the operation of complex processes, mostly when large datasets are available. Moreover, the review on that subject showed very little studies on the application of ANN

models to perform the comparison of similar equipment as a tool to identify and improve process issues.

1.1 Thesis Objectives

The present work proposes simulation models for the PECEM power plant steam generator and cooling tower based on operation data through artificial neural networks.

The specific objectives of the study are meant to:

- Employ ANN associated to statistic assessment;
- Investigate ANN as a tool for problem detection.

1.2 Thesis Outline

This work is composed by three independent chapters. Chapter 1 provides a review on the applications of ANN for power plant and related subjects, together with correlated approaches. ANN was evaluated when used in power plant process and equipment. Chapter 2 brings the development of an ANN trained to estimate the steam mass flow rate generation of a real coal-fired power plant, based on past records of its operation. ANN configuration is obtained after a series of tests aiming to reduce the prediction error, which are then compared to a reference multiple linear regression model. Chapter 3 presents ANN models capable of estimating the water makeup and heat rejection of a wet cooling tower. These models can estimate tower outputs with high accuracy for similar equipment even under different operating conditions.

2 A REVIEW ON THE APPLICATION OF ANN TECHNIQUES FOR POWER PLANT MODELING

2.1 Introduction

The raising share of renewable sources on electric power generation forced energy matrix worldwide to diversify. However, thermoelectric power plants remain important to guarantee the electric base load, and research on that field looks forward to identify appropriate operational strategies, efficiency enhancement and to adequate plant operation to the cohabitation with power generation from renewable sources. That scenario lead to the development of tools, such as artificial neural networks, able to handle with complex system integration, based on real data.

This chapter aims to present a review on the application of artificial neural networks ANN to power plant equipment, with a special interest on steam generators and cooling towers. Attention was given to present up-to-date practices related to steam generators and wet cooling towers modeling.

2.2 Artificial neural networks

Artificial neural networks (ANNs) are inspired by the functioning of a biological neural. In other words, ANN is an attempt to reproduce the human brain functioning. ANNs resemble the human brain because they acquire knowledge of the network from the environment through a learning process and use synaptic weights to store the acquired knowledge [Haykin, 2001]. However, it is noteworthy that the artificial neurons currently developed are primitive when compared to brain neurons, able to reproduce the functioning of the human brain [Haykin, 2009].

2.2.1 History

The first work related to ANNs was proposed by McCulloch and Pitts, in 1943, who presented an analogy between living cells and electronic processes, simulating the behavior of a neuron. Their model did not present a learning law, which was proposed by Hebb in 1949.

Hebb demonstrated that the network learning potential depends on the activation of pre and post synaptic cells, that once simultaneously activated lead to a change in synaptic weight.

In 1958, Rosenblatt suggested the perceptron model with the objective of training an ANN to obtain greater synaptic efficiency. Minsky, in 1969 proved that the perceptron model was not able to solve the so called XOR problem since it is a non-linearly separable problem. Since then, studies related to artificial neural networks were reduced due to a lack of perspective in the development of the subject.

However, Rumelhart, Hinton and Williams, in 1986, developed a training method called backpropagation algorithm for the training of neural networks based on the use of multi-layer perceptron. This algorithm enabled the resolution of more complex problems with the use of neural networks [Haykin, 2001], and studies on ANNs and their applications gained a new impetus, but they declined again in the 1990's due to configuration and convergence issues for solving high complexity, and also due to the competition of new algorithms.

Finally, in 2006, Hilton et al proved the ability to train highly complex deep learning networks without convergence problems. Currently, deep networks continue to be developed, aiming to improve the performance of networks in the area of forecasting and regression. Despite the revolution caused by deep networks, they require massive amounts of data to achieve good performance and are not suitable for all types of problems.

2.2.2 Brief description

ANNs are composed of simple processing units, the neurons, which are able to compute mathematical functions. Neurons compose the layers. Layers connections are associated with weights that weighted ANN entries.

The ANN learning phase is the beginning of the problem-solving process that will be solved. In the learning process, the weights of the connections are adjusted until they are able to represent the problem

A feed-forward ANN is composed of a set of artificial neuronal processors or elements distributed in layers, interconnected by one-way communication channels. The end of these channels of communication occurs through the synapses between the neurons [Silva Neto and Becceneri, 2009].

Haykin, 2009, defined three basic elements of a neuron: synapses, summing and activation function, as schematically presented in Figure 2.1.

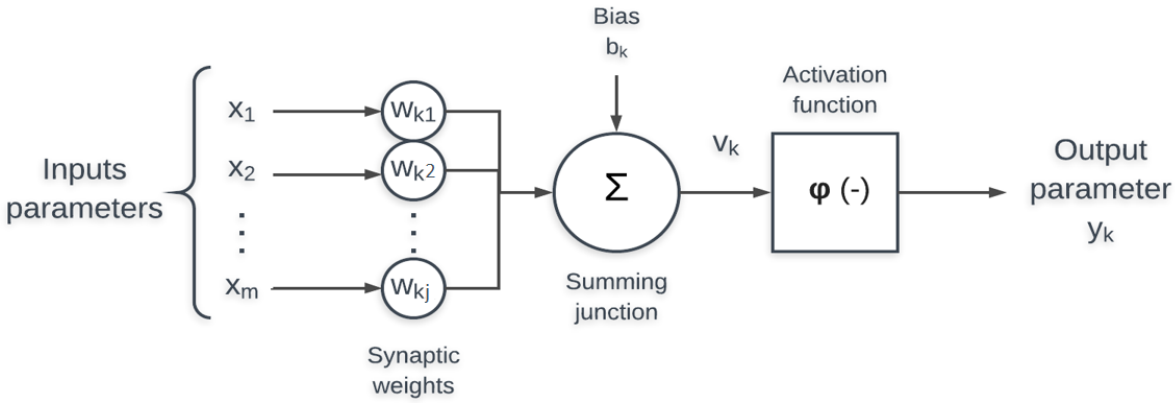

Figure 2.1 – Artificial Neuron proposed by McCulloch and Pitts [Adapted from Haykin, 2009].

For a given neuron v_k, an input signal x for a synapse j is multiplied by the synaptic weight w_{kj}. Different from the weight of a biological process, the synaptic weight of an artificial neuron can have both negative and positive values. The adder, Σ, is responsible for summing the set of input signals, weighted by their synaptic forces of each neuron k. The activation function limits the neuron output amplitude, described in detail in section 2.2.5.1 [Haykin, 2009].

It is also possible to mathematically describe the functioning of a neuron with Equations 2.1 and 2.2.

$$v_k = \sum_{j=1}^{m} w_{kj} x_m \tag{2.1}$$

$$y_k = \varphi(v_k + b_k) \tag{2.2}$$

The sum of the products of inputs x to their weights w results in the linear combined output v. The second Equation gives the output signal of the neuron, y, which depends on the previous result from v, the bias b and the activation function φ. It should be noted that bias is the polarizing parameter, which increases or decreases the intensity of the input signal uniformly.

Neural networks are characterized by parallel search and content addressing, where there is no memory address or search for information in sequence; learn from experience; association of different patterns; generalization; abstraction and robustness [Silva Neto and Becceneri, 2009].

The processing of an ANN occurs in a similar way to the learning process that occurs with humans. ANN learning process takes place in two stages, training and execution [Gevrey et al., 2003]. In training, ANN is exposed to and based on a dataset, it identifies which information is relevant to going through the learning process. In this stage, the weight of the connections between the neurons is defined [Mohanraj et al, 2015; Silva Neto and Becceneri, 2009].

2.2.3 Learning process

The concept of learning in the ANN context can be defined as a process by which non-pre-set parameters of a network are influenced by a process of stimulation based on the environment in which the network is inserted. Learning can vary according to the modification of environment variables [Mendel and McLaren, 1970]. There are two common learning methods in neural networks, known as supervised and unsupervised learning. What differs from these methods is the knowledge or not of the output data, the answers to the problem [Lecun et al., 2015; Mohanraj et al, 2015; Silva Neto and Becceneri, 2009].

Supervised learning can be compared to learning with a teacher, as shown in Figure 2.2. From the concept that the teacher has the information about the environment when both, the teacher and the student, are exposed to the environment for a training, the teacher will know the correct result. This information is then transferred to the network, and the training process goes on iteratively until the error signal is sufficiently low. The error signal represents the difference of the value obtained by the network with the real value, that is, the value informed by the teacher.

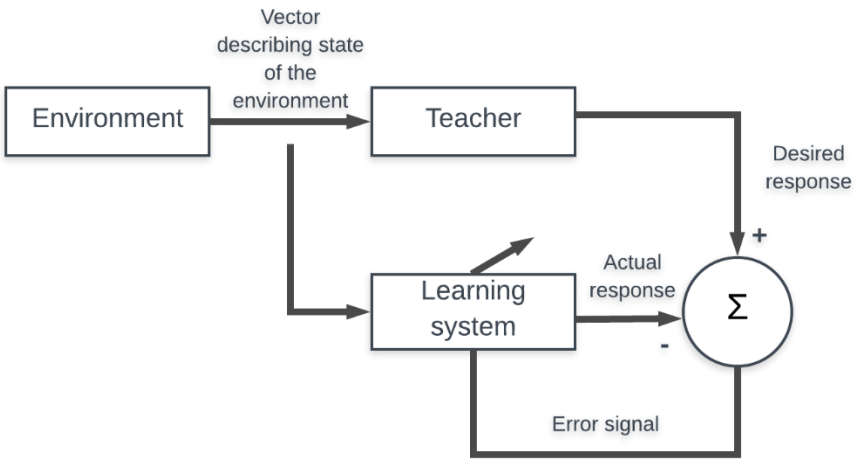

Figure 2.2 - Diagram of the supervised learning method [Adapted from Haykin, 2001].

Supervised learning is based on error correction, its performance is usually measured by the mean square error or the sum of the square errors of the training sample. In order for the error to become smaller, and as network learning improves, it must achieve a local minimum or the global minimum of the error surface. This error surface movement is based on the examples presented for the system and the systematic correction of the weights in the synapses of the neurons, following the descending gradient method (described in section 2.2.5.2). This prevents the network from learning randomly [Haykin, 2009].

Another possibility for learning is unsupervised, which is divided into two subcategories, reinforced learning, and unsupervised learning. Reinforced learning requires input and output parameters, as well as supervised learning, but its learning process takes place through interaction with the environment, where learning happens by observing the time sequence of the stimuli formed by the process [Haykin, 2009]. Non-supervised learning, on the other hand, allows us to approach problems where the desired result is not known. Thus, a non-supervised network aims to determine standards, characteristics or categories according to input data presented to the network [Silva Neto and Becceneri, 2009].

2.2.4 ANNs architecture

There are basically two classes of network architectures: non-recurrent and recurrent networks. The non-recurring is those that only feed the input data and can be classified as: single-layer or multi-layer fed networks [Haykin, 2001]. Recurrent networks are those that have a feedback process, where the outputs of the neurons are used as input signals to the other neurons [Silva Neto and Becceneri, 2009].

The architecture of an ANN is summarized by the number of layers, number of neurons in each layer and the type of connection between neurons. These variables are dependent on the type of problem to be solved, so it is necessary to observe the best architecture for a given situation. For example, a single layer ANN composed of a neuron between the input and output layers can be used only for linearly separable problems [Haykin, 2001].

There are no rules to define the best configuration according to the problem. It is important to define a sufficient number of neurons and hidden layers to avoid unnecessary training and to achieve the best performance. The dataset has the best generalization performance can be reached by evaluating the ANN error [Kavzoglu, 1999].

2.2.5 Multiple layer perceptron

The perceptron network is a model composed by one layer of input neurons and another one by output neurons. Whenever intermediate layers are added, the model is called multilayer perceptron (MLP), which is an extension of the perceptron model, proposed by Rosenblatt. It is composed of several intermediate or hidden layers of artificial neurons [Gevrey et al., 2003; Silva Neto and Becceneri, 2009]. Figure 2.3 shows a schematic representation of the MLP architecture.

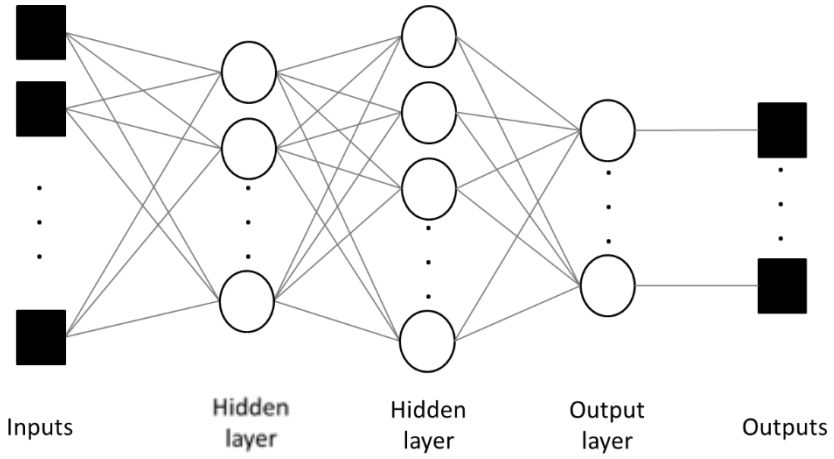

Figure 2.3 - Perceptron Architecture of Multiple Layers.

Inputs are associated to neurons in the input left hand layer, where the outside information feeds the network. As a next step, information passes to the hidden layer to be processed. Processed information is transferred to the output layer, the right hand and final layer.

The MLP model stands out for three characteristics, nonlinear activation function, hidden neurons and a high degree of connectivity [Haykin, 2001]. The activation function must display a smooth non-linearity so that there is gradient variation and the error is reduced. Hidden neurons are responsible for the absorption of progressive knowledge, thus enabling the execution of more complex tasks. Finally, it is important to emphasize that the network has high connectivity and that any modification in the network requires it to be restructured [Haykin, 2001].

2.2.5.1 Activation function

The activation function is responsible for modulating the information generated by the neuron, and must be used by multiple layers artificial neurons in the perceptron method. Its main purpose is to ensure the non-linearity of the model, thus allowing ANN to learn and perform more complex tasks. The most known activation functions are linear and sigmoid.

The sigmoid function represents a linear and non-linear behavior, as shown by the logistic function (Equation 2.3) and the hyperbolic tangent function (Equation 2.4).

$$\varphi(v) = \frac{1}{1 + \exp(-av)} \tag{2.3}$$

$$\varphi(v) = \tanh(v) \tag{2.4}$$

where a is the slope parameter of the function. The hyperbolic tangent function (Equation 2.4) allows negative values to be assumed by bringing analytical benefits.

2.2.5.2 Backpropagation

The backpropagation algorithm presents an operation described by Haykin, 2001, that begins with the initialization, where it is assumed that the network has no previous information, followed by examples of training, early computation, inverse computation and iteration.

The backpropagation algorithm is based on the descending gradient method that computes the partial derivatives of an error function considering the weight vector of a given input vector. In an ANN with more than one input, the network function has as many arguments as the number of inputs, then the partial derivate is computed for each argument [Rojas, 1996].

The following sections aim to present a review of ANN applications to model power plant equipment such as steam generators and wet cooling towers are discussed as a closure.

2.3 ANNs applied to steam generators

Steam generators are complex heat exchangers, which produce water vapor under pressures greater than atmospheric from the thermal energy of a fuel and an oxidizing

element, air [Torreira, 1995]. It is worth mentioning that, in most cases, the steam generator is the system responsible for generating steam in thermoelectric plants, where the steam is used to generate electric energy through the turbines. In general, steam generators are composed of the following components: furnace, boiler, superheating fluids, economizer and air heater. Figure 2.4 schematically shows a steam generator [Bazzo, 1995].

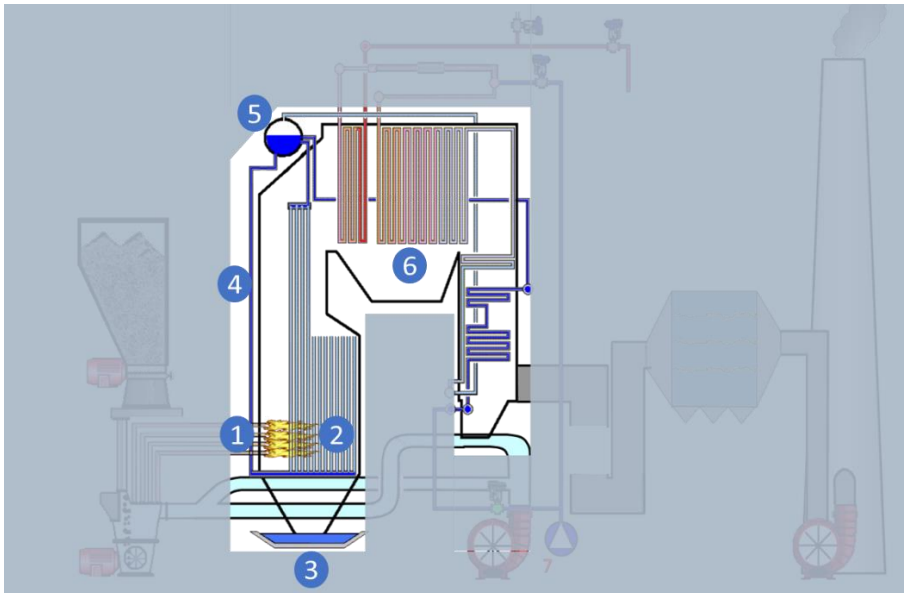

Figure 2.4 - Schematic representation of a steam generator.

Fuel (1) is burned in the furnace or the combustion chamber (2). During the combustion process, heavy ashes fall and settle to the bottom in the furnace (3) where they are collected and generally used in the cement industry. The light ashes are carried by the gasses, upwards towards the superheaters (6). The boiler comprises the parts where the phase change of water from the liquid state to the vapor occurs. The water walls (4) and the drum (5) are part of the boiler. The water circulates freely by density difference and the formed vapor is accumulated in the upper part of the drum. The steam is saturated and from there is directed to the superheaters (6). The superheater is designed to increase the temperature of the steam generated in the boiler by absorbing energy by radiation and by convection [Bazzo, 1995].

Despite the simplified explanation of the operation of steam generators, these devices have complex functions, as well as the control and maintenance of steam generators. Power plant maintenance affects the efficiency of the process. Due to this, the importance of planning and prevention of maintenance in the power plants. In addition to avoiding

equipment losses, there is a reduction in the need for plant shutdowns, which result in a power outage and higher power consumption for startup of power units [Kopanos et al., 2018].

In the last two decades, several studies have emerged evaluating the accuracy of neural networks to estimate or predict steam generator parameters [Deshpande et al., 2012; Estiati et al., 2016; Fast and Palmé, 2010; Ghugare et al., 2014; Li et al., 2002; Mesroghli et al., 2009; Nowak and Rusin, 2016; Oko et al., 2015; Smrekar et al., 2009; Strušnik and Avsec, 2015; Strušnik et al., 2015; Suresh et al., 2011; Tunckaya and Koklukaya, 2015a, 2015b].

ANNs have a wide range of application, ranging from problems involving some kind of association that must be established within a set of references or benchmarks, with many data or variables, to problems where the parameter correlations are hard to stablish [Dave and Dutta, 2014].

Li et al., 2002, demonstrated the potential of the application of neural networks in the control of thermoelectric power plants. Initially, an ANN was trained to learn the steam generator dynamics for given burning rates and turbine valve positions. The number of intermediate layers and their neurons was determined from the test by evaluating the performance of the neural networks. The sigmoid function was used in the intermediate layers and a linear function in the output layer, with the backpropagation method. Authors have proved the good performance of the networks to estimate fluid pressure and energy production of the steam generator.

Mesroghli et al., 2009, evaluated the coal gross calorific value (GCV) from 25 US sites with regression approaches and ANNs. The aim of the paper was to answer three general questions. Firstly, the possibility to generate relationship between parameters of analysis of the GCV for different coal samples, followed by the possibility of increasing the accuracy of the classification, and finally the comparison of ANNs with regressions in respect to the performance of GCV estimation. Input parameters were normalized to increase the efficiency of the network training. Three neural networks were assembled and authors chose to use feed-forward ANNs with error backpropagation mechanism and the sigmoid logistic function as the activation function. Authors showed that the regression performance was superior because of the linear relationship between the input and output parameters, although ANN performance was satisfactory.

Smrekar et al., 2009, developed a study of the application of the ANN models to estimate the steam mass flow, pressure and temperature of a coal-fired steam generator, based on actual plant operating data. Authors evaluated the performance of two neural networks,

where the input parameters were varied. Data was pre-treated and the relation among parameters was assessed. Feed-forward ANN was used with the error-propagation mechanism as an intermediate layer with 22 neurons and a hyperbolic tangent as the activation function. Both models presented three input parameters, two of which are identical, valve openings at the outlet of the boiler and pressure of the feed water at the outlet of the valve, and displayed low error values when estimating vapor properties. The first model presented a mean error of 0.95, 0.38 and 0.47% for flow, temperature and pressure, and 1.35, 0.39 and 0.48% for the second model, considering the same parameters. Since their errors were very close, it was concluded that the two models can estimate the steam properties of a coal-fired steam generator.

Fast and Palmé, 2010, developed a set of integrated ANNs, where each modeled a thermoelectric plant component as a basis for actual operating data. The developed networks were multilayer perceptron type with an intermediate layer and as the hyperbolic tangent function as the activation function. Four models were developed: gas turbine, heat recovery, steam generator and turbine. Model performances presented parameter prediction errors of less than 1% in most cases. This study allowed for plant optimization, as well as the advancement of its maintenance with economic benefits.

Suresh et al., 2011, developed a model for a real thermoelectric plant with the aim of optimizing its parameters. An association of methodologies was used, including neural networks. The developed ANN indicated the lowest required energy for plant operation. Two scenarios were studied, with and without water feedback, with a 0.9999 R^2 and 0.9728. The study showed the ANNs' ability to predict the desired output with backpropagation with Levenberg-Marquardt learning algorithm and an intermediate layer with four and six neurons.

Deshpande et al., 2012, presented a comparative study of two types of neural networks, backpropagation (BProp) and radial baseS (RB). These models were used to evaluate the performance of coal-fired power plants by evaluating their heating rate and efficiency of the steam generator through actual operating data. Two ANNs were developed for each configuration. RP network was assembled with two intermediate layers, ten neurons each. The BR network used an intermediate layer with 219 and 162 neurons for the steam generator heating rate and efficiency. In both cases, BProp network presented better performance with R^2 of 0.91 and 0.964 the former outputs.

Ghugare et al., 2014, studied the ability of an artificial ANN to predict higher heat values (HHV) of biomass fuels based on the difficulty predicting HHV for non-homogeneous

fuels. Authors developed two ANN models with different input parameters to estimate HHV. Both neural networks used the sigmoid function as a transition function and the linear function on the output layer. Finally, ANN models were still compared to genetic algorithm (GA) models to evaluate the performance of each methodology for HHV ranges (low, medium and high values). ANN and GA models can be compared for one of the cases but ANN displayed a higher performance for the second one (ANN R^2 of 0.907, 0.844 and 0.838 and GA R^2 of 0.843, 0.825 and 0.751.

Oko et al., 2015, applied neural network modeling to estimate the pipe pressure and water level of a coal-fired power plant. Database was generated after simulations. The work resulted in an ANN NARX with three input parameters and two output parameters, two intermediate layers, with 100 neurons each. Authors emphasized the ANN training process, stressing the importance of data pre-processing, avoiding excessive network training, overtraining, and post-processing network exit data. It also presented ANNs ability to estimate the output parameters, even if the input parameters show sudden changes.

Strušnik and Avsec, 2015, analyzed turbine control valves and heater throttling valves of a combined heat and power system. They proposed three ANNs combined in a fuzzy logic algorithm for control. ANNs presented R^2 values very close to 1, and the mean square error was 1.82, 1.47 and 2.49 for each ANN. The same ANNs were used to optimize the use of the heater and thus use the plant in a more rational way.

Strušnik et al., 2015, presented a study with real data of an energy generator. Two ANN were developed aiming to estimate steam generation and its efficiency. Authors found very close values for efficiency, with 90.722% for the actual measurement and 90.018% for ANN.

Tunckaya and Koklukaya, 2015a, presented a comparative study of ANN performance with two other methodologies, linear multiple regression and integrated autoregressive moving average from real operating data. The purpose of the study is to predict the rate and production of a coal-fired thermoelectric plant. All methodologies presented good performance with R^2 above 0.927 and RMSE lower than 0.3353. However, the best performance was achieved with the use of the artificial neural network with R^2 equal to 0.992 and RMSE equal to 0.164. It is noteworthy that the study had 37 input parameters to determine the plant production rate.

Tunckaya and Koklukaya, 2015b, conducted a similar study to predict NOX emission, and found low performance for all the proposed models, due to the database small sizes.

Estiati et al., 2016, evaluated the performance of an ANN in estimating biomass higher heat value, based on literature values. ANN performance was compared to regressions for three scenarios, and found better results for ANN.

Nowak and Rusin, 2016, developed an ANN to estimate the steam temperature at a turbine inlet. That parameter was used to assess machine operation for power generation and provide support for decision making. A metamodel based on two ANNs was developed and presented results with errors around 20%. Authors suggested to increase the size of the data set for the training of the models in order to enhance the model accuracy.

Table 2.1 shows a summary of the studies described above comparing their applications, the data set characteristics used, the ANN model and type, and the learning algorithm used.

Table 2.1 – Review of papers using ANN for problems involving steam generators.

Reference	Application	Output	Data	Architecture	Network type	Learning algorithm
Li et al., 2002.	Power plant boiler	Throttle pressure and megawatt	Operation data	5-5-5-1 5-11-11-1	MLPNN	BProp
Mesroghli et al., 2009.	Gross calorific value of coal	Gross calorific value (GCV)	Real plant data	3-10-1 6-10-1 7-10-1	FFNN	BProp
Smrekar et al., 2009.	Fresh steam properties on coal-fired boiler	Pressure, temperature and mass flow rate of steam produced	Real plant data	3-22-3	FFNN	BProp
Fast and Palmé, 2010	Heat and power plant	Combined heat and power plant components	Operation data	4 inputs and 9 outputs (Gas turbine) 6 inputs and 6 outputs (HRS) 2 inputs and 3 outputs (Boiler) 7 inputs and 3 outputs (Steam turbine)	MLPNN	LM
Suresh et al., 2011.	Coal-fired supercritical power plant	Minimum heat input	Simulated data	5-4-1 5-6-1	MLPNN	LM
Deshpande et al., 2012.	Thermal power plant	Heat rate and boiler efficiency	Real plant data	9-10-10-1 (Heat Rate) 9-219-1 (Heat Rate) 5-10-10-1 (Boiler efficiency) 5-162-1 (Boiler efficiency)	MLPNN	BProp RB
Ghugare et al., 2014.	Higher heat value of biomass fuel	Higher heating value of solid biomass fuels	Theoretical data	3-5-3-1 5-6-4-1	MLPNN	BProp
Oko et al., 2015.	Coal-fired subcritical power plant	Drum pressure and level	Simulated data	3-100-2	NARXNN	LM

Strušnik and Avsec, 2015.	Heat and power system in thermal power	Steam enthalpy and entropy	Simulated data with supply information from plant operation	2-60-10-2 2-35-5-2 2-80-2	FFBP	LM
Strušnik et al., 2015.	Boiler steam generator	Electrical power, industrial steam power, thermal power 1 and 2, thermal plant efficiency, gross power	Real plant data	1-20-8-2-4 1-60-10-2	FFBP	LM
Tunckaya and Koklukaya, 2015a.	Coal-fired power plant	Coal-fired power plant production rate	Real plant data	37-12-1	FFBP	LM
Tunckaya and Koklukaya, 2015b.	Coal-fired power plant	NO_x emissions	Real plant data	8-24-1	FFBP	LM
Estiati et al., 2016.	Higher heating value of biomass fuel	Higher heating value	Theoretical data	3-7-1	FFBP	LM
Nowak and Rusin, 2016.	Steam turbine heating	Steam temperature at the turbine inlet	Theoretical data	6-25-11-3 9-7-4-3-1	FBNN	BProp

Based on the above review, it can be observed that there is a wide application of ANNs in problems involving steam generators. The supervisory system enables these to be performed on steam generators from the data set of the operation of that equipment. This makes it possible to model equipment with a high complexity of the operation.

2.3.1 ANNs applied to steam generators bibliometric

The articles presented in section 2.3 were analyzed in relation to the year of publication, as shown in Figure 2.5.

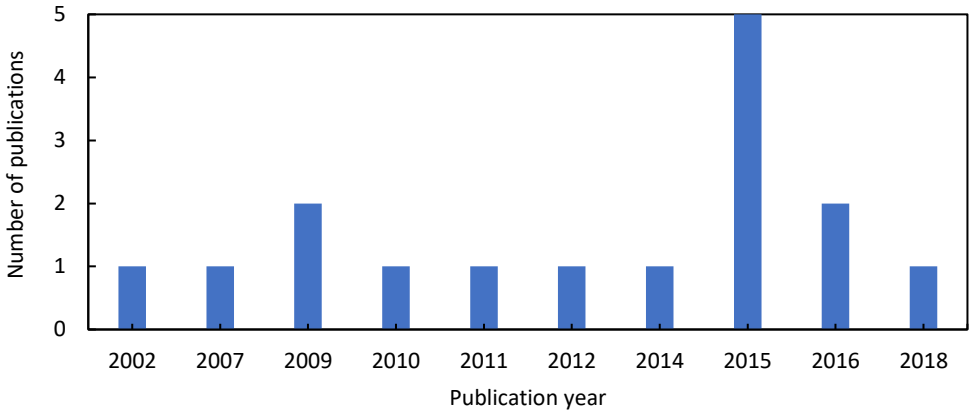

Figure 2.5 - Bibliometrics: Publications years of steam generator studies.

It is possible to observe that studies related to the use of the neural network for modeling of steam generators and the like have been occurring in the last 15 years proving the efficiency of the methodology in modeling these types of equipment. In addition, there has been an increase in the application of neural networks in recent years in works related to steam generators. Figure 2.6 illustrates the type of data set used in the studies presented in the previous section. In addition, the methodology used to evaluate the performance of the models.

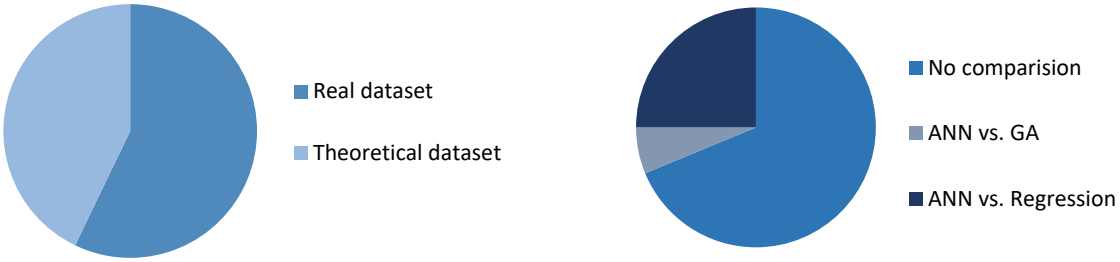

(a) (b)

Figure 2.6 – Bibliometrics of (a) Steam generator articles dataset; (b) Steam generator articles models comparison.

Based on the evaluated works, it was noticed that for the modeling of equipment related to the steam generator, both simulated databases and actual operating data are used. For me, most of the studies used some methodology to compare the performance of the neural network model developed for the study.

2.4 ANNs applied to wet cooling towers

Cooling tower is heat-withdrawal equipment from a stream of water to atmospheric air with consequent water cooling [Cooling Tower Institute, 2007]. Its thermal performance is vital for industrial units and small deviations from design specifications can lead to serious implications for the operation and economy of a process [Jasiulionis, 2012]. Figure 2.7 shows a schematic view of the water and air counter flows of a wet cooling tower.

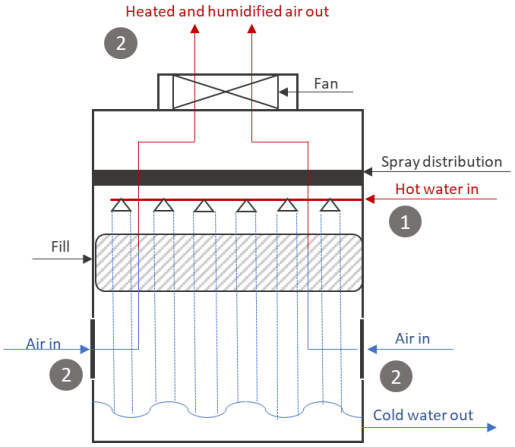

Figure 2.7 - Direct contact or open evaporative cooling tower schematic view [Adapted from ASHRAE, 2016].

Water cooling is done by a combination of heat and mass transfer. Hot water is distributed in the tower by spray nozzles (1), splash bars or films, thereby increasing the ratio of exchange contact surface to volume of the droplets. Atmospheric air circulates through fans (2), convection current, natural wind current or spray induction effect. A fraction of water absorbs heat to change from liquid phase to vapor at constant pressure, which is the main source of heat exchange.

Modeling involves heat and mass transfer phenomena of both air and water streams, with complex interactions. Accurate analytical or numerical modeling aims to reproduce wet cooling tower behavior with different accuracy levels. However, some operation issues are not easily modeled, like decreasing capacity, leakages, and environmental changes. Several studies emphasized these limitations, thus justifying the use of models based on Artificial Neural Networks ANN [Cortinovis, 2009a; Jasiulionis, 2012; Qi et al., 2016; Wu et al., 2018].

Hosoz et al., 2007, trained an ANN with experimental data obtained from a countercurrent cooling tower operating on a steady state to predict the performance of a cooling tower. The model was able to predict the rejected heat, the evaporated water rate, the process water outlet temperature, the dry bulb temperature and the relative humidity of the outlet air. Correlation coefficients between simulated and experimental data were predicted to range from 0.975 to 0.994, as well as the mean relative errors was found to lie between 0.89% to 4.64%.

Good results were also found by Qasim and Hayder, 2017, who trained an ANN from acquired data from an experimental cooling tower, obtaining correlation coefficients in the range of 0.913 to 0.985 and mean relative errors in the range of 1.22% to 6.01%.

Qi et al., 2016, developed an ANN model to predict the performance of shower cooling towers with the use of wavelets activation functions, obtaining good results between experimental data and simulated data in the range of 0.990 to 0.998 for the coefficient of correlation and 1.39% to 2.28% for the mean relative error.

With the objective of developing an ANN based controller for evaporative capacitors, Abbassi and Bahar, 2005, obtained good results in ANN training for prediction in transient and steady state regimes of the evaporated water mass flow rate, dry bulb temperature and specific humidity air outlet temperature from the condensing temperature of the refrigerant fluid, massive flow of refrigerant, air inlet temperature, specific inlet moisture and water mass flow rate.

Gao et al., 2013, and Mahdi et al., 2014, trained ANNs to predict natural draft and to predict the effects of wind direction and velocity on the performance of hyperbolic cooling towers with satisfactory results.

According to the literature review, it can be stated that ANN is an appropriate methodology to model and simulate wet cooling towers whenever experimental data are available.

2.4.1 ANNs applied to cooling towers bibliometric

Figures 2.8 and 2.9 illustrate the frequency of published work in relation to neural network application in cooling towers over the last 13 years. Moreover, the data set used to carry out the study.

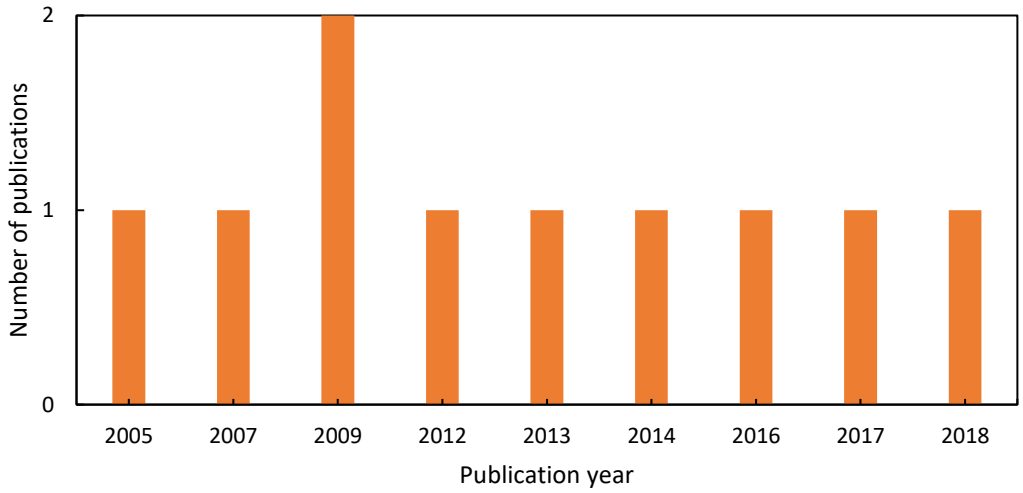

Figure 2.8 – Bibliometrics: Publications years of cooling towers studies.

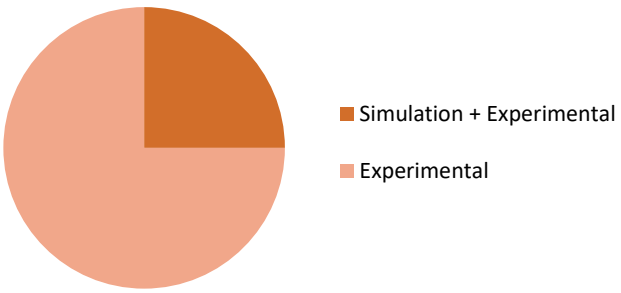

Figure 2.9 – Bibliometrics of cooling tower dataset.

According to the studies evaluated, they allow concluding that an application of artificial neural networks for cooling tower modeling has been performed in the last 13 years. This shows that the methodology has been applied constantly due to the good performance of the methodology in modeling cooling towers. However, as shown in Figure 2.9, the set of data used for the development of the model refers to experimental data or simulated data. This analysis allows concluding the lack of cooling tower models based on actual operating data.

2.5 Dataset

The dataset used in this study refers to the operation log of two identical thermoelectric power plants. The plants have a generation capacity of 360 MW each. The operating condition of each plant varies between 240 MW and 360 MW according to the demand of the electric system. The data sets are composed of measurements of operational parameters of the plant over a one-year hourly average. The data set was randomly reorganized for the statistical analyses and for the development of linear multiple regression and artificial neural network models.

For the development of the linear multiple regression model, we chose to divide the data set into training and testing. For the development of the artificial neural network model, the data set was divided into three groups, training, testing and validation.

it was decided to model the steam generator and the cooling tower due to its relevance to the operation of the plant.

2.6 Conclusions

Literature review pointed out that ANNs are powerful tools to model real equipment as steam generators and wet cooling towers with significant benefits. That approach has already been employed since the last 20 years for different situations. Some studies also propose the use of more than one methodology for developing models capable of estimating complex behavior of real equipment. It came clear that the use of ANNs is effective in improving power plant efficiency, and they should be considered as a helpful tool for improving system control and operation.

3 STEAM FLOW ESTIMATION WITH ARTIFICIAL NEURAL NETWORK BASED ON POWER PLANT OPERATIONAL DATA

3.1 Introduction

Thermoelectric power generation stands for 24.5% of the Brazilian electricity matrix [ANEEL, 2019], and improvements on its operating efficiency are important to enhance system availability and reliability with less environmental impact. The development of better control and monitoring techniques is constantly done by power generation developers and stakeholders. Steam generation is a multi-parametric process and its modeling involves coupled phenomena. This complexity associated with the available access to important amounts of continuous operation data from supervisory systems makes this problem particularly suitable to machine learning models. Machine learning models such as artificial neural networks (ANN) are able to recognize patterns and to infer relationships from complex sets of data.

ANNs have already been successfully applied to reproduce and simulate the behavior of heat transfer problems involving gas modeling, optimization of energy efficiency and NO_x emissions, forecasting of energy resources, among others [Ghugare et al., 2014]. Specific ANN models were proposed by [De et al., 2007; Smrekar et al., 2009; Strušnik et al., 2015] to simulate real power plants and their equipment.

De et al., 2007, present the development of an ANN model for the biomass and coal cofired CHP plant. The developed model is found to quickly predict the performance of the plant with good accuracy with 1.93% of maximum error in estimating the power output. Smrekar et al., 2009, examine the feasibility of ANN modeling for coal-based power or combined heat and power (CHP) plants. The developed model can model the power plant with average errors of around 1%. Strušnik et al., 2015, modelled a boiler and found an efficiency increases by 0.704%, representing 1960 tons of coal consumption saving, and consequently, 5628 tons of CO_2 emissions reduced.

The objective of this work is to present the development of an ANN model to estimate steam generation of a coal-fired power plant. The model is based on a real operational database of the PECEM [1] power plant (2x360 MW of rated capacity). Records of steam flow rate and pressure, fuel flow rate and water temperature at the steam generator inlet, primary,

[1] www.energiapecem.com.br

secondary and over-fired air flow, oxygen level and wet bulb temperature for several periods and operation conditions were used.

This study evaluates the performance of ANNs and regression models in respect to performance parameters for different operating conditions. Furthermore, fine tuning procedures regarding the ANN training structure were done with the aim to decrease the estimation error.

3.2 Problem description

PECEM power plant generates 720 MW of electricity with two similar size power groups, equipped with coal-fired superheated steam generators (SSG), each one designed to produce 360 MW with 1200 t/h of superheated steam at 540ºC and 18MPa. Figure 3.1 presents the SSG schematic layout and displays the set of input and output parameters.

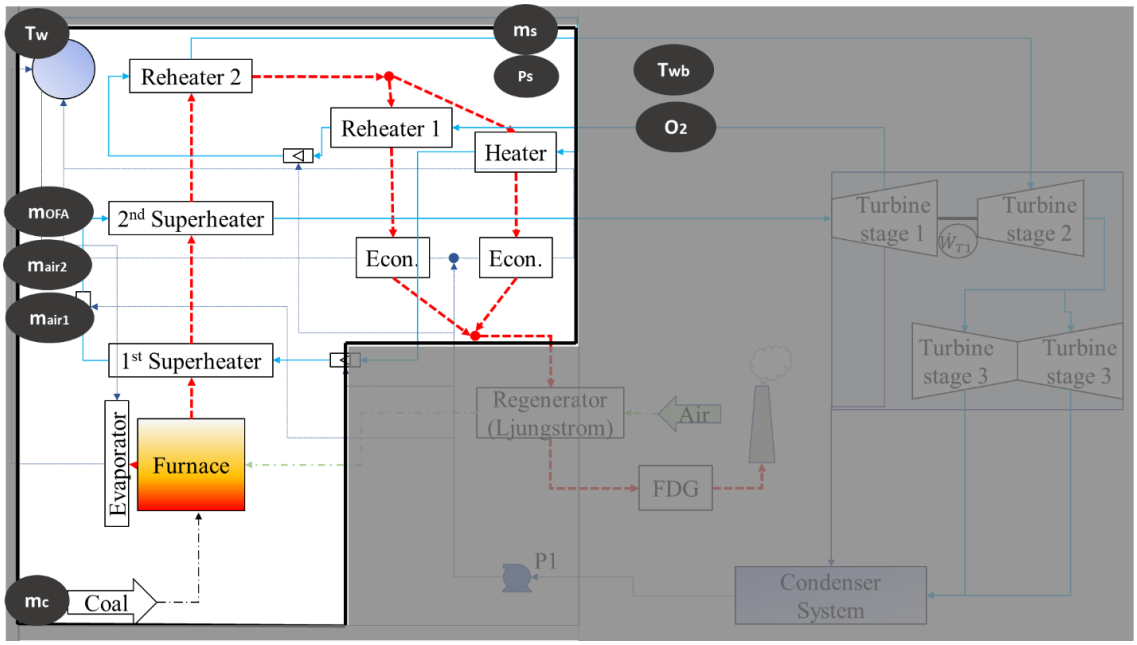

Figure 3.1 – PECEM Superheated Steam Generator SSG

Input parameters were selected from a yearlong dataset, allowing the identification of two separate power plant electric output regimes, at 240 MW and 360 MW, imposed by the national electric grid operator[2] (ONS). Steam generation mass flow rate $\dot{m}_s$ was chosen as the parameter to be estimated by the ANN, based on the SSG inlet water temperature T_w, steam

[2] ://ons.org.br

pressure steam P_s, coal mass flow rate $\dot{m}_c$, primary air flow $\dot{m}_{air1}$, secondary air flow $\dot{m}_{air2}$, over fire air flow $\dot{m}_{OFA}$, oxygen O_2 and wet bulb temperature T_{wb} . Reference values for those parameters are displayed in Table 3.1.

Table 3.1 – SSG parameters and their ranges

Parameter	Abbreviation	Minimum	Maximum
Water temperature	T_w	168.41 ºC	279.10 ºC
Steam pressure	P_s	0.799MPa	18.54 MP
Coal mass flow rate	$\dot{m}_c$	0.923 t/h	149.81 t/h
Primary air flow	$\dot{m}_{air1}$	12.30 kg/s	97.07 kg/s
Secondary air flow	$\dot{m}_{air2}$	106.24 kg/s	281.61 kg/s
Over fire air flow	$\dot{m}_{OFA}$	6.04 kg/s	69.37 kg/s
Oxygen	O_2	0.69%	16.63%
Wet bulb temperature	T_{wb}	17.71 °C	27.86 °C
Steam mass flow rate	$\dot{m}_s$	0.803 t/h	1285.63 t/h

These minimum and maximum values were based on the supervisory dataset and assumed as reference boundaries of the SSG operation.

3.3 Methodology

The present section aims to describe a step-by-step sequence of actions, or methodology, applied to estimate the SSG steam mass flow rate $\dot{m}_s$. The methodology was developed in four blocks due to the problem complexity. Block 1 (Figure 3.2) refers to the data processing.

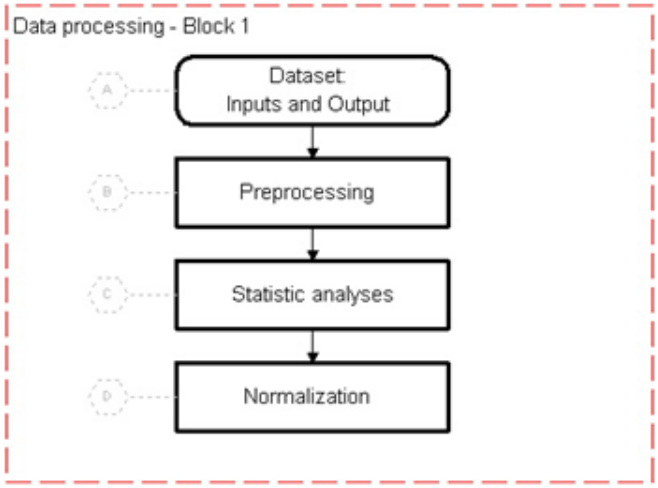

Figure 3.2 –Block 1- Data processing

Dataset (letter A) refers to parameters presented in Table 3.1. The preprocessing procedure (letter B) is dedicated to data cleaning, as the original data source can present defective values, like zeros and negative numbers. Faulty data were replaced by interpolated adjacent values as this is a recommended practice (Han et al., 2012).

Statistic analyses (letter C) perform assessments based on correlations to understand the relationship between the parameters. An important outcome is to identify whether data are part of a time series by searching for correlations based on timesteps. The Pearson correlation index was used to assess the mutual influence between parameters (Table 3.2). The upper diagonal was leaved blank due to the matrix symmetry.

Table 3.2 –Dataset Pearson correlation index for the SSG parameters from Table 3.1 for the plant yearlong dataset

	Water temperature (T_w)	*Steam pressure* (P_s)	*Coal mass flow rate* ($\dot{m}_c$)	*Primary air flow rate* ($\dot{m}_{air1}$)	*Secondary air flow rate* ($\dot{m}_{air2}$)	*Over fire air flow rate* ($\dot{m}_{OFA}$)	*Oxygen* ($O_{2)}$	*Wet bulb temperature* (T_{wb})	***Steam mass flow*** ($\dot{m}_s$)
Water temperature (T_w)	1								
Steam pressure (P_s)	0.96	1							
Coal mass flow rate ($\dot{m}_c$)	0.96	0.96	1						
Primary air flow rate ($\dot{m}_{air1}$)	0.72	0.65	0.74	1					
Secondary air flow rate ($\dot{m}_{air2}$)	0.86	0.90	0.90	0.49	1				
Over fire air flow rate ($\dot{m}_{OFA}$)	0.27	0.27	0.21	0.07	0.10	1			
Oxygen ($O_{2)}$	-0.60	-0.52	-0.47	-0.54	-0.27	-0.18	1		
Wet bulb temperature (T_{wb})	-0.15	-0.18	-0.07	0.05	-0.06	-0.22	0.10	1	
Steam mass flow ($\dot{m}_s$)	**0.98**	**0.99**	**0.96**	**0.66**	**0.90**	**0.29**	**-0.55**	**-0.18**	**1**

Table 3.2 last line displays the steam mass flow rate Pearson correlation index, ranging from 1 (best values) to 0 (poor correlation) in absolute value. Steam pressure showed to be the highest correlated parameter in respect to steam mass flow rate, followed by water temperature, coal mass flow rate and secondary air flow. Input parameters also displayed high cross coefficients, showing that they also are strongly correlated. Wet bulb temperature and over fire air flow did not present strong correlation with steam mass flow. These same correlations can be graphically seen in Figure 3.3.

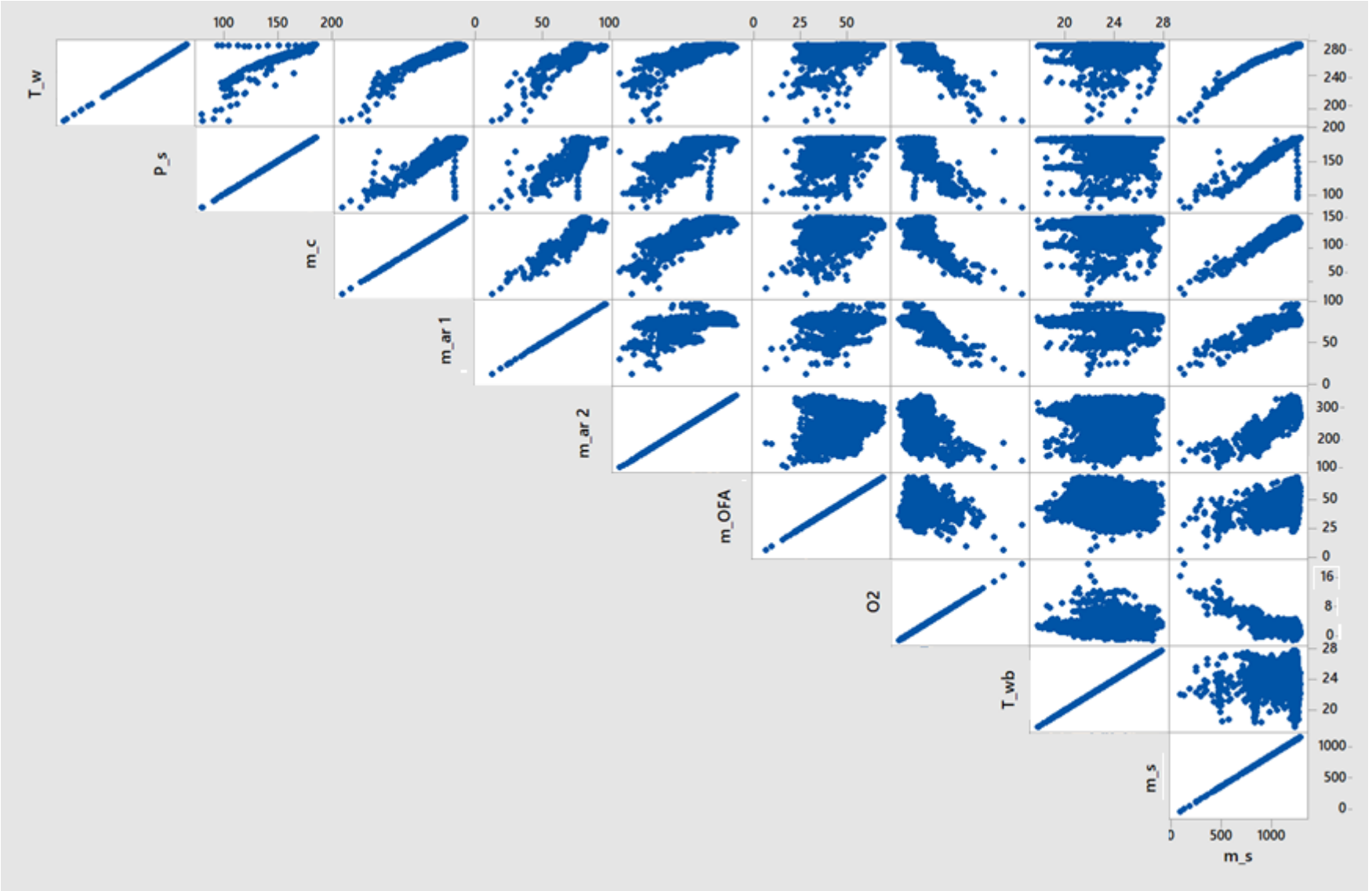

Figure 3.3 – Steam generator correlation matrix.

Figure 3.4 presents the sequence of actions to obtain results from linear multiple regression (Block 2), followed by results from ANN (Blok 3), that are compared in Block 4.

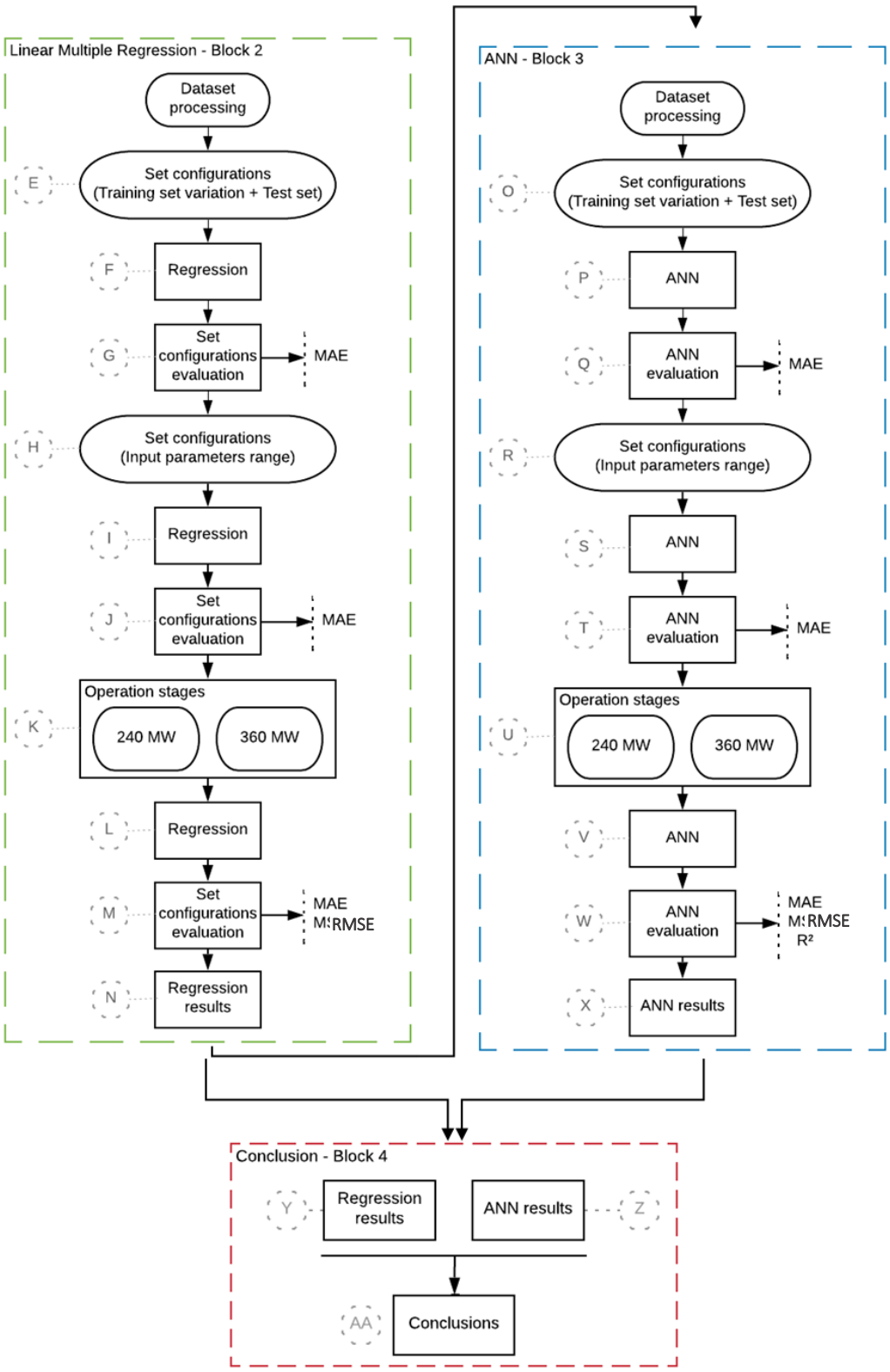

Figure 3.4 – Methodology scheme for Linear multiple regression (Block 2), ANN (Block 3) and Conclusions (Block 4)

Diverse set configurations were assembled with dataset processed in letter E; Block 2, each one built upon a particular training and testing partition. The test group was fixed with 1489 samples, 20% of the dataset, and the training group ranged from 1489 to 5957 samples, or 20% to 80% of the dataset. The variation of training group size allows the decision making of the best set configuration to develop the ANN model. A reference model was built based on linear regression with all set configurations (letter F).

Linear regression evaluation was performed in letter G (Set configurations evaluation) based on the Mean Absolute Error MAE, calculated by Equation 3.1 with data from the test group.

$$MAE = \left(\frac{1}{n} \sum_{i=1}^{n} |X_{est} - X_{obs}| \right) \tag{3.1}$$

with X the steam mass flow rate for both measured (obs) and estimated (est) values and n the number of data points.

After the training dataset evaluation (letter G), the number of input parameters was downgraded from 8 to 3 input parameters, (letter H), and the model performance was evaluated in letter I with the same criterion.

PECEM power plant concentrates its operation on two electric power output levels, as presented in Figure 3.5.

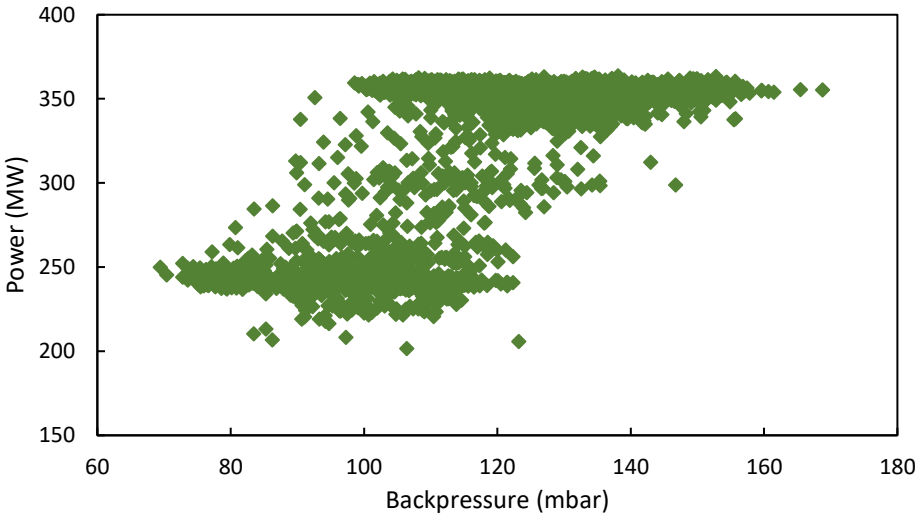

Figure 3.5 – PECEM electric power output levels as a function of the vapor condensation pressure

Dataset with operational conditions concerning the mean value of 240 MW and 360 MW were prepared in letter K. The intermediary points were disconsider as they stand for transitional operation. The regression model performance was evaluated once more by their Mean Absolute Error MAE but also by their Root Mean Squared Error RMSE (letter L), the former calculated by Equation 3.2.

$$RMSE = \sqrt{\frac{1}{n}\sum_{i=1}^{n}(X_{est} - X_{obs})^2} \tag{3.2}$$

RMSE penalizes large errors values, while the MAE evaluates the absolute error, without differentiating individual error weights.

Block 3 presents the ANN development methodology. The processed dataset was also divided into training and test group to evaluate the best set configuration (letter O; Block 3). All set configurations were used to build ANNs, evaluated by their Mean Absolute Error MAE in order to identify the best set configuration. (letter Q). The number of input parameters was evaluated, in letter R, and the best ANN architecture was defined, in letter T, throughout MAE and RMSE. After the definition of the inputs number, the dataset was divided into the operational states (letter U), 240 and 306 MW. ANN evaluation for each operation stage (letter V) was made by calculation of MAE, RMSE and R^2 (Equation 3.3) for the evaluation of each ANN developed in relation to the observed values of steam flow.

$$R^2 = \left(1 - \frac{\sum_{i=1}^{n}(X_{obs} - X_{est})^2}{\sum_{i=1}^{n}(X_{obs})}\right) \tag{3.3}$$

ANN Multi-Layer Perceptron MLP type was chosen to simulate the SSG, which is an extension of the perceptron model proposed by Rosenblatt, built with several intermediate or hidden layers of artificial neurons (Gevrey et al., 2003; Silva Neto and Becceneri, 2009). MLP model comprehends intermediary neurons, responsible for the absorption of progressive knowledge, enabling the execution of more complex tasks. Finally, it is worth emphasizing that the ANN has high connectivity since any modification in the neural network requires a restructuring (Haykin, 2001).

The network architecture and parameters had to be set: activation function; the number of hidden layers; the number of neurons in each layer; the number of inputs to be used; and the amount of data to be used in the training of the ANN. Figure 3.6 shows the ANN architecture used in this work.

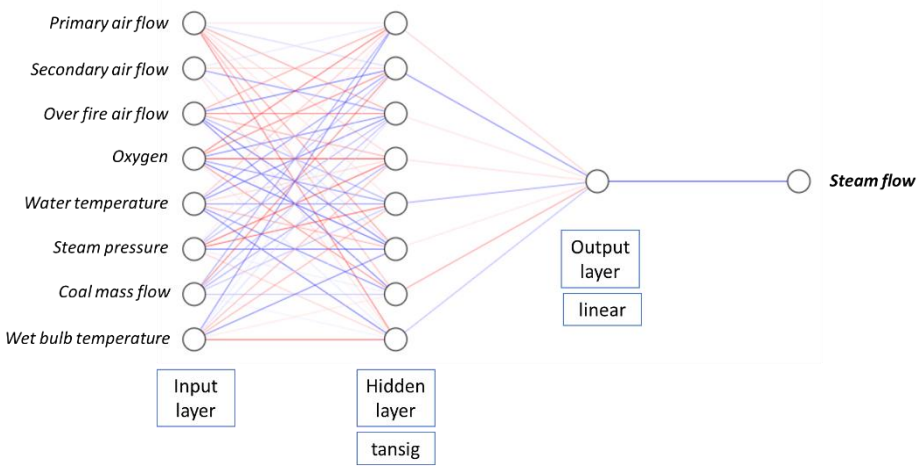

Figure 3.6 - ANN architecture developed for steam flow estimation

The input parameters are presented at the first layer in Figure 3.6. Hidden layer and the number of neurons needed to be set are also shown. That step was evaluated by trial and error by changing the number of neurons and the consequent RMSE and MAE values for each individual ANN. Sigmoidal hyperbolic tangent function, *tansig*, was set as the transfer function. The output layer with the steam mass flow rate in this architecture holds one only neuron and the linear function was used as the transfer function. The ANN multilayer feed forward perceptron with backpropagation mechanism was chosen, together with *trainlm* (Levenberg-Marquardt back propagation) as the training function. The Matlab *nntool* was used to develop the ANN. Error assessment were performed with the aid of Minitab and Excel.

3.4 Results and discussion

3.4.1 Linear Multiple Regression

Estimation of the steam mass flow rate $\dot{m}_s$ based on real data from PECEM power plant, as described in Table (3.1) can be represented by Equation (3.4),

$$\dot{m}_s = f\left(T_w,\ P_{s,}\ \dot{m}_c,\ \dot{m}_{air1},\ \dot{m}_{air2},\ \dot{m}_{OFA},\ O_2,\ T_{wb}\right) \quad (3.4)$$

and followed the steps of the proposed methodology, whose application is described in this section. The consolidated dataset prepared in Block 1 became the input for the calculation of linear multiple regressions along Block 2. Results were assessed by means of their Mean Squared Error RMSE and the Mean Absolute Error MAE (letter G). Figure 3.7 presents the evaluation of regression accuracy in respect to the training data size.

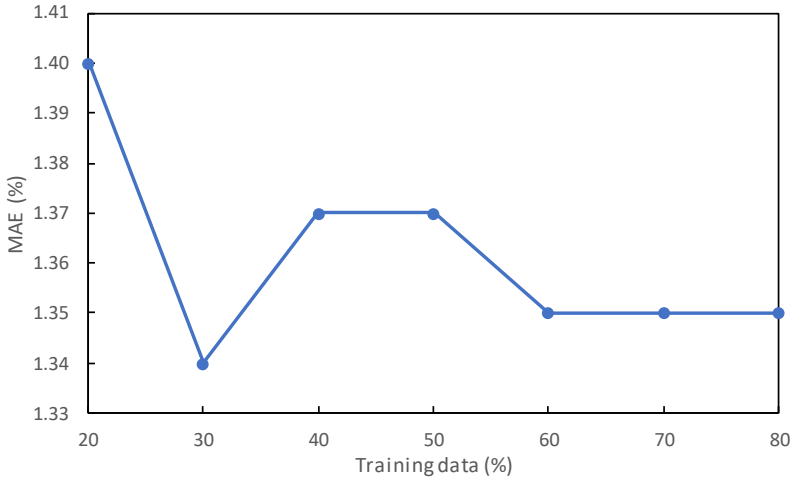

Figure 3.7 – Regression evaluation for training data size

Calculated MAE values ranged from 1.34 to 1.40, a narrow variation that does not allow to conclude witch training data size displayed the best performance. Complementary MAE calculations were performed (letter H) in respect to the number of input parameters of the linear multiple regressions, as shown in Figure 3.8.

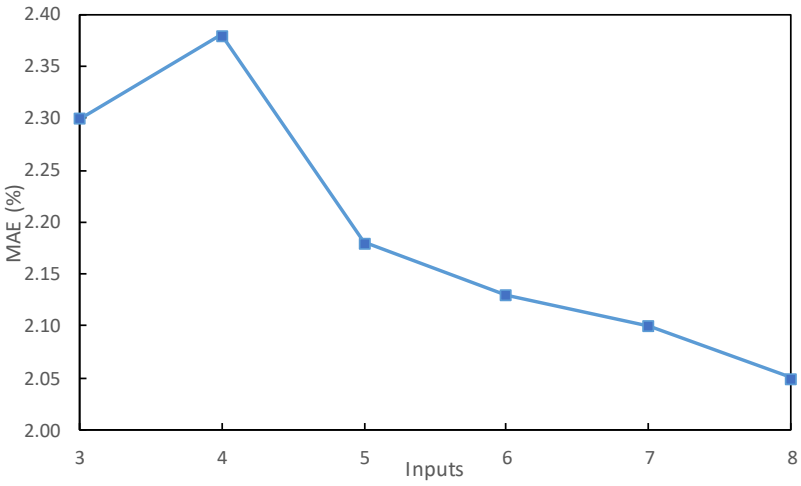

Figure 3.8 – Regression evaluation for number of inputs

Training data size was built with 70% of the dataset and remaining 30% were left for the testing procedure. The best performance was achieved with MAE of approximately 2.0% for 8 inputs (letter J), but its difference from the worse one, with a calculated MAE close to then 2.4 % for 4 inputs, can be seen as a close result.

The correlation index between the input and the output parameters helped to decide which input parameter could be excluded, once lower Person index values means that the relation between the parameters are low. In one hand, the smaller the number of input parameters, the less information is transmitted to the model, but in this particular case the exclusion of some input parameters did not significantly increase the error.

Finally, the dataset was divided into two groups according to the power generation level, 240 MW and 360 MW (letter K), although the transitional stage was also evaluated, as presented in Table 3.3 (letter M).

Table 3.3 – Regression evaluation for operation levels and stages

#	Regression	RMSE (%)	MAE (%)
1	360 MW_8 inputs	25.21	15.43
2	360 MW_3 inputs	30.13	17.76
3	240 MW_8 inputs	11.32	9.47
4	240 MW_3 inputs	11.54	9.29
5	Transitional_8 inputs	7.19	5.31
6	Transition_3 inputs	8.06	6.06
7	Overall dataset_8 inputs	2.92	2.05
8	Overall dataset_3 inputs	3.35	2.3

Best results were found for regressions built out from the larger dataset (#7 and #8), followed by the ones for the transition stages. It is possible to observe an increase of the error values with the restriction of the output power range. Thus, it can be inferred that restricting the range of operation increases the complexity of the problem as the noise of the input-output variables starts to become important and the problem itself becomes less linear. As a consequence, the regression model presented higher error values since it became less able to characterize the relation between the input-output variables. (letter N).

3.4.2 Artificial Neural Network

The same assessment was performed with the ANN approach. Seven set configurations with particular ranges for the input parameters (Table 3.4) were evaluated to choose the training data size (letter O), as shown in Figure 3.9.

Table 3.4 –Set configurations with particular ranges for training data size

#	Training data size	Test data size
1	20% (1489)	
2	30% (2234)	
3	40% (2978)	
4	50% (3723)	20% (1489)
5	60% (4468)	
6	70% (5212)	
7	80% (5957)	

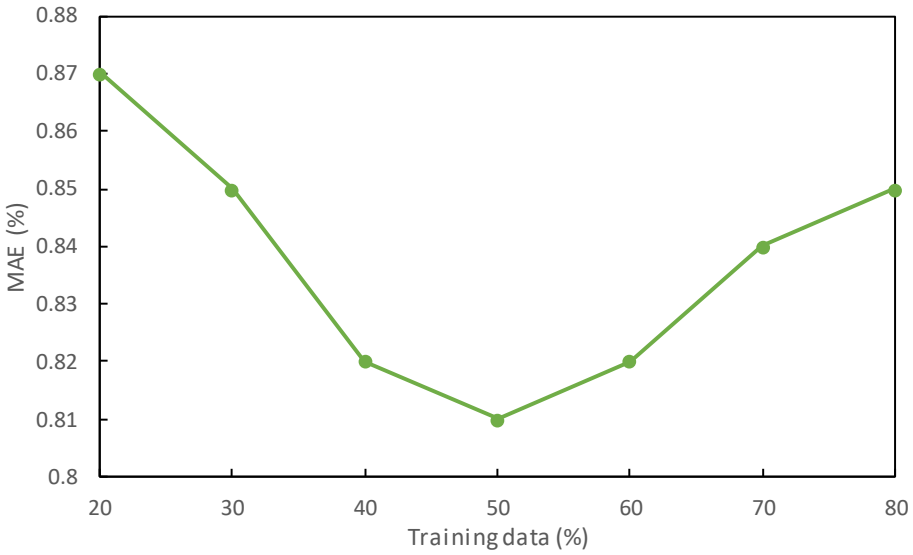

Figure 3.9 – ANN evaluation for each set configuration as a function of the training data size

MAE values shown that the training data size had negligible effect on the model performance. Thus, the configuration chosen was the same as used for linear multiple regression, 70% of the dataset for training and 30% for test.

The steam mass flow rate ANN architectures were also assessed in respect to their number of neurons and hidden layers. Four different architectures built with the complete dataset were compared and evaluated by their RMSE values, as presented in Table 3.5.

Table 3.5 – Steam mass flow rate ANN architectures performance with the complete dataset

#	Architectures	RMSE (%)	MAE (%)
1	ANN_8_8_1	1.59	1.175
2	ANN_8_16_1	13.37	1.207
3	ANN_8_8_8_1	1.60	1.188
4	ANN_8_16_16_1	1.63	1.193

The lowest RMSE and MAE values were found for architectures with two intermediate layers and 8 neurons in the first one and one in the last hidden layer (ANN #1), although the remaining networks presented similar error values. Thus, the ANN chosen to the next evaluations steps is ANN #1.

Figure 3.10 presents the ANN performance in respect to the number of input parameters.

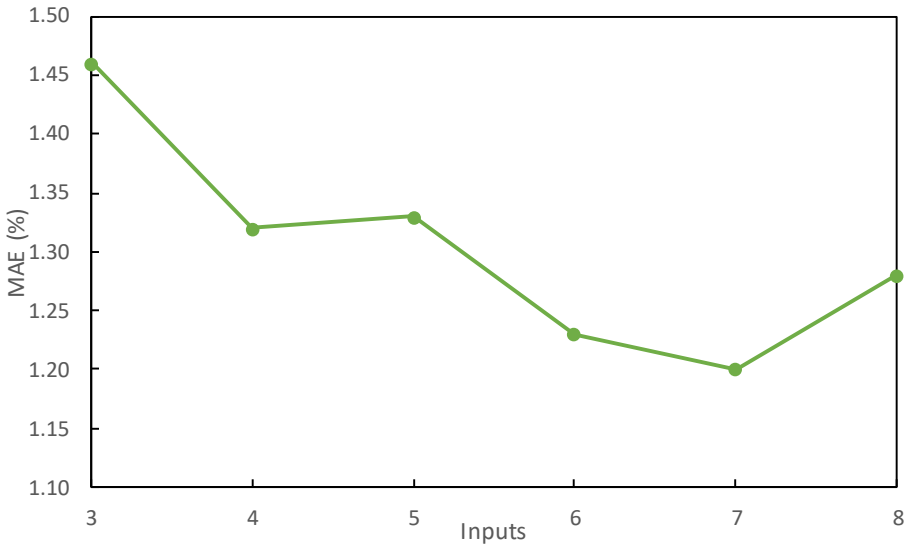

Figure 3.10 – ANN performance in respect to the number of inputs

The variation of the number of inputs did not present significant difference of their MAE values. Based on that assessment, the following steps were performed with both three and eight input parameters.

Finally, the dataset was separated into two operational electric output power levels, 240 MW and 360 MW, presented in Figures 3.11 and 3.12.

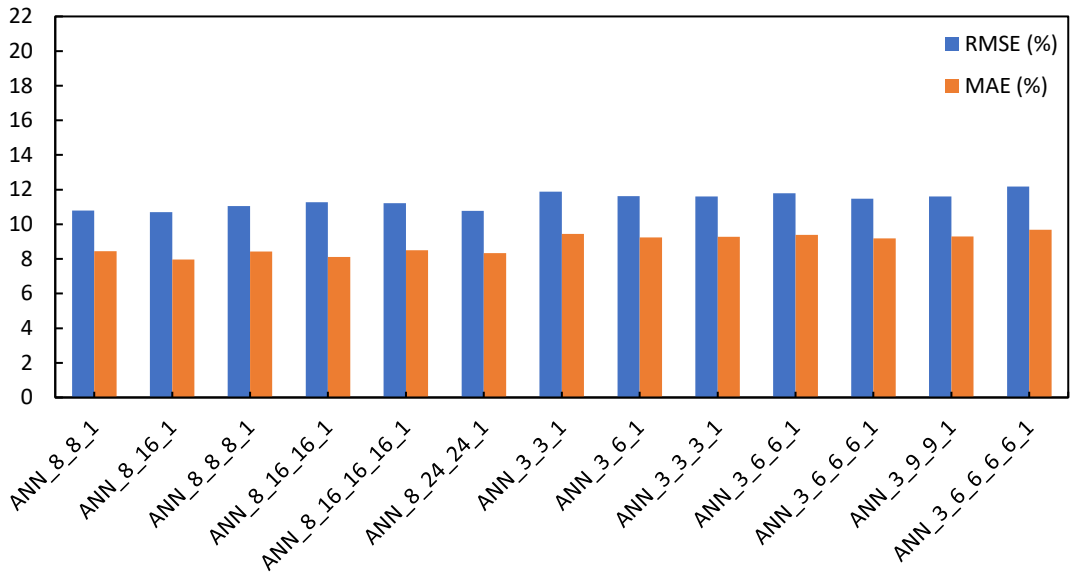

Figure 3.11 – Calculated errors RMSE and MAE for several ANN with data from plant 240 MW power output.

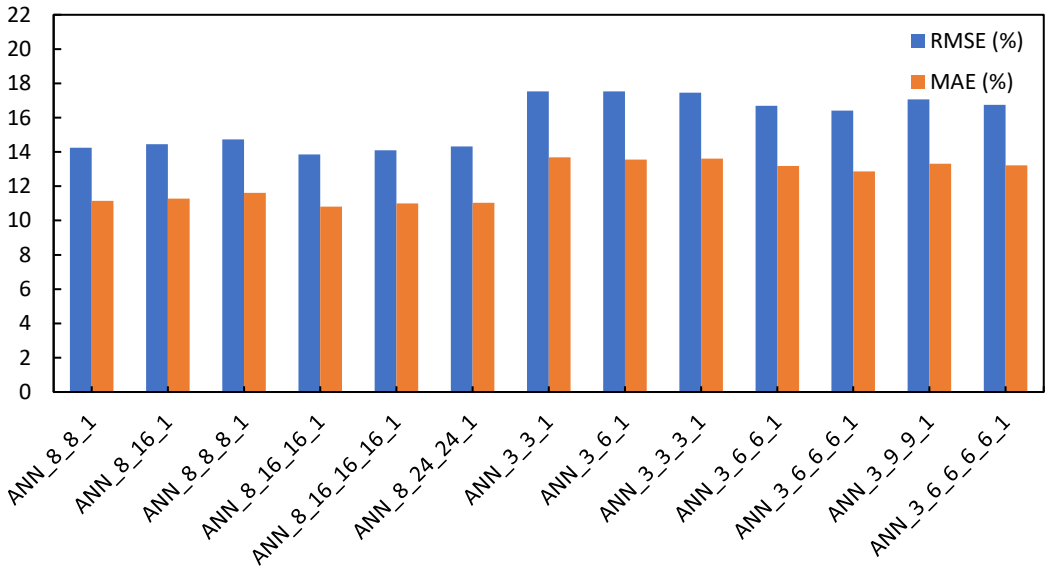

Figure 3.12 – Calculated errors RMSE and MAE for several ANN with data from plant 360 MW power output

The best ANN architecture with eight inputs for 240 MW electric output was found with two hidden layers, sixteen neurons in the first one and one neuron in the last hidden layer (ANN_8_16_1). The best architecture for the model with three inputs is composed by four hidden layers, with six neurons in the first three layers and one in the last layers (ANN_3_6_6_6_1).

The best ANN with eight input parameters for 360 MW electric output was found with three hidden layers with sixteen neurons in the first two layers and one neuron in the last neuron (ANN_8_16_16_1). However, for the same power level with three input parameters, the best ANN is formed by four intermediary layers with six neurons each and one neuron in the output layer (ANN_3_6_6_6_1).

When comparing the performance of each model to the two 240 and 360 MW ranges, errors, RMSE and MAE, are higher for the 360 MW range. For the transition study the architectures evaluated are presented in Table 3.6.

Table 3.6 – Steam mass flow rate ANN architectures errors for the transition stage

#	ANN	RMSE (%)	MAE (%)
1	ANN_8_8_1	6.66	4.85
2	ANN_8_8_8_1	7.42	5.15
3	ANN_8_16_1	7.25	5.68
4	ANN_3_3_1	6.74	5.17
5	ANN_3_6_1	6.24	5.02
6	ANN_3_3_3_1	6.54	5.21
7	ANN_3_6_6_1	6.11	4.19
8	ANN_3_6_12_1	6.32	5.00
9	ANN_3_6_6_6_1	6.14	4.76

The best architecture for eight input parameters was ANN #1, composed of two intermediate layers with eight neurons each and one neuron in the output layer, and the best one for three input parameters was ANN #7, with by two intermediary layers with six neurons each and one neuron in the output layer. Table 3.7 presents the ANN models summary for each operation stage and number of inputs.

Table 3.7 - ANN evaluation for operation stages

ANN	RMSE (%)	MAE (%)	R^2
360 MW_8 inputs	13.85	10.82	0.87
360 MW_3 inputs	16.69	13.19	0.80
240 MW_8 inputs	10.28	8.11	0.91
240 MW_3 inputs	11.47	9.18	0.89
Transition_8 inputs	6.66	4.85	0.99
Transition_3 inputs	6.11	4.91	0.99
Overall dataset_8 inputs	1.76	1.28	0.99
Overall dataset_3 inputs	1.99	1.46	0.99

After completing the best ANN architecture for each specific set configuration, these models were compared to their respective regressions, as shown in Figure 3.13 to verify which one displayed the best capacity to estimate the generated steam mass flow rate.

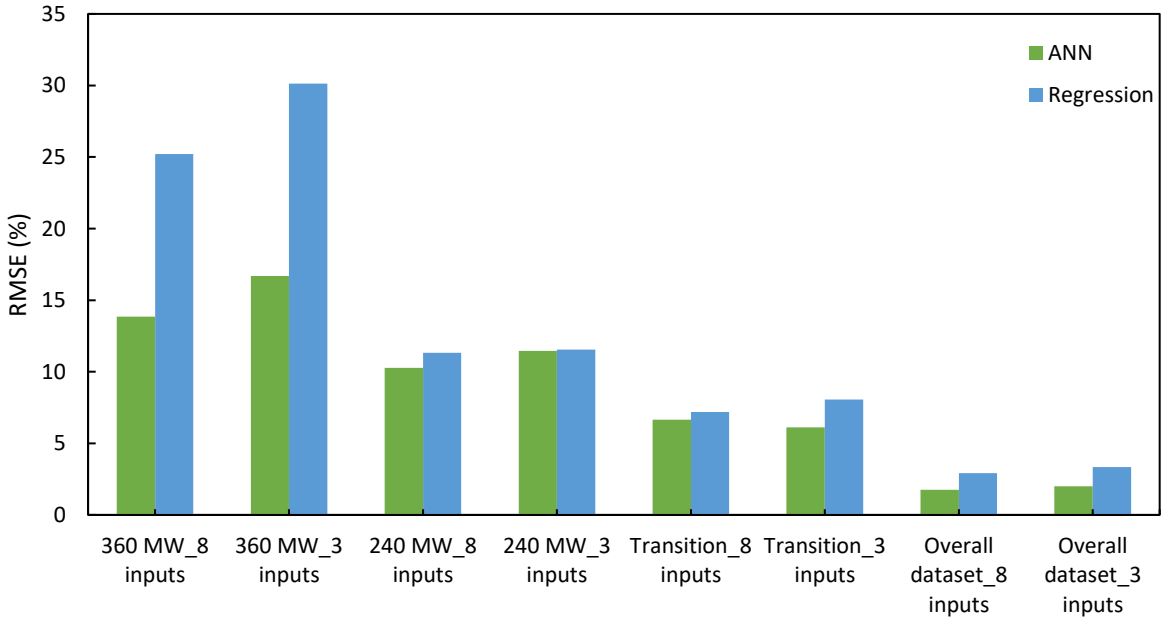

Figure 3.13 - ANN and regression RMSE for selected models

ANN models presented lower RMSE values than their respective regressions. Higher errors were found for the 360 MW power level, for both ANNs and regressions. Best results were found for the complete dataset, composed by data from 240 up to 360 MW. The 360

MW power level error was estimated to be around 15 %, followed by errors of 10% for the 240 MW power level, 5% for the transition regime, and less than 3% whenever the complete set of data was used to build the neural networks. ANN models were likely more efficiency to reproduce the problem profile than regression when the problem does not present a profile.

The correlation coefficient of the models confirms the best performance of the models for the total dataset and transition range, followed by 240 MW and 360 MW power level. These results affirm the best ANN performance when presenting a data set with a more evident linear profile of the operation.

Since the regression RMSE values were much higher than the ones for the ANN models, the ANN models were used to evaluate the describe the steam generator operation. As an example, the actual steam mass flow rate of 1093.4 t/h was compared to both regression and ANN outputs, which resulted in estimated values of 1114.0 t/h and 1088.2 t/h, respectively, or 20.6 t/h and 5.16 t/h deviation in respect to the reference value.

3.5 Conclusions

The aim of this study was to develop ANNs models capable of estimating the steam mass flow rate from a steam generator of a coal-fired power plant, based on acquired data. Linear multi variable regression models were built and compared to the neural network. Different combinations of training group sizes, number of inputs and the operation levels or regimes were set to be investigated.

The effects of these combinations must be evaluated for each regression and ANN model, as they brought complexity to the problem. The best ANN architecture for the eight-input combination was made of two hidden layers with sixteen neurons in the first hidden layer and one neuron in the last layer for 240 MW and three hidden layers with sixteen neurons in the first two layers and one neuron in the last neuron for 360 MW. The best-performing ANN the three-input combination was found to be made of two hidden layers, six neurons in the first one and one in the last for 240 MW and four intermediate layers, six neurons in the first three layers and one in the last for 360 MW.

All evaluated combinations displayed lower MAE and RMSE values for ANN models then for regressions. For overall dataset with the combination with eight inputs that difference became unimportant whenever the models were built from the complete dataset, with ANN RMSE and MAE of 1.76% 1.28% respectively in contrast with RMSE and MAE of 2.92% and 2.05%. Segregated datasets for 240 MW or 360 MW presented better results than the ones

from regression, as they displayed errors approximately 50% larger for the 360 MW power output level complete dataset and transition regime displayed similar low error responses.

Based on these error assessments, it became possible to conclude that the ANN models were able to estimate steam mass flow rates based on actual data with better results than the ones from regression models.

4 PERFORMANCE ESTIMATION OF A COOLING TOWER USING AN ANN MODEL

4.1 Introduction

Heat rejection to the environment is a key factor to guarantee thermal power plant performance. Among several types of available equipment, wet cooling towers appear as a suitable option due to their high heat rejection capacity as they operate at wet bulb temperature level, allowing to enhance plant efficiency. Research and development actions toward the improvement of the equipment capacity and operational conditions are though justified as they can impact other factors besides fuel consumption efficiency.

The power plant working fluid has its temperature lowered after the contact with atmospheric air, in a combined heat and mass transfer interaction. Convective exchange is added to water evaporation, in a large contact surface area. The main contribution to promote water cooling is given by the partial evaporation of water, accounting for 80% of the water temperature reduction [Cortinovis et al., 2009a, 2009b].

Cooling towers are classified according to the type of air circulation and can be natural, induced or forced. Natural air circulation towers, or atmospheric towers, the upper part of the equipment is closed to compel the air to circulate in the horizontal direction, ensuring its cross flow while water is sprayed from the top. The cooling tower is free of auxiliary power to induce air flow but displays large drag losses. Induced air circulation tower operates with fans to promote air flow, placed at the top of the equipment, so the air flows vertically from bottom to top, while water is distributed from the top, in a counter current flow. This type of tower presents greater thermal exchange efficiency, but need external power to operate. And finally, the forced airflow towers, where the fans are positioned in the air inlet at the bottom of the equipment. Thus, the air circulates from the bottom up, increasing the efficiency of the heat exchange, however, the fans have higher powers [Jasiulionis, 2012].

The removal of heat from the plant occurs through the cooling of the fluid through the exchange of heat with atmospheric air [Cooling tower institute, 2007]. Cooling towers are responsible for lowering the temperature of the water and this occurs through a combination of heat mass transfer. Process water is exposed to an area with a large contact surface with atmospheric air. Figure 4.1 shows the temperature relationship between water and air in counterflow cooling towers.

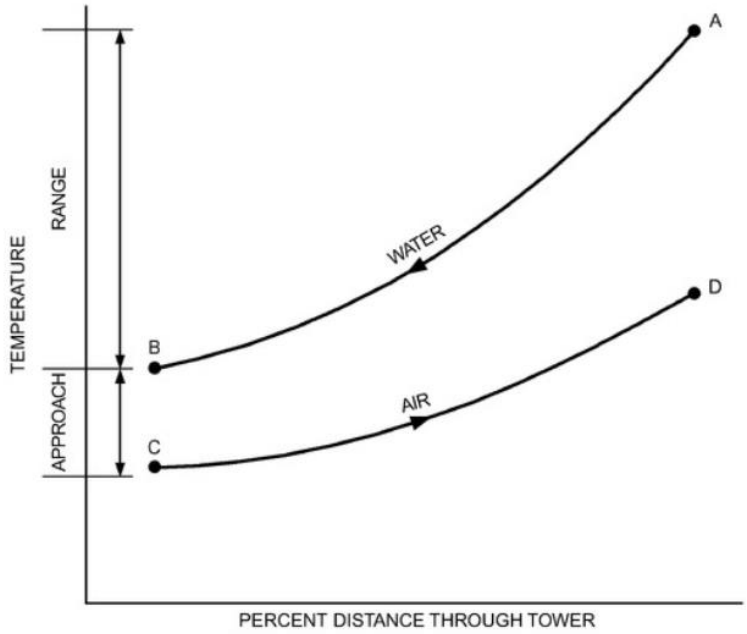

Figure 4.1 - Counterflow cooling tower operation [ASHRAE, 2016]

Figure 4.1 shows the reduction of water temperature (A to B) consecutively the humid temperature of the air increases (C to D). The difference between the water temperature at the exit of the cooling process and the air temperature at the inlet of the process is called the approach. The approach is related to the cooling capacity of the cooling tower. The range is known for the difference in water temperature at the inlet and outlet of the process. The thermal performance of the cooling tower is mainly dependent on the wet bulb temperature at the process input.

In a cooling tower, the main contribution to cooling the water is given by the evaporation of part of the water. Evaporation accounts for 80% of the water temperature reduction. The remaining 20% refers to the temperature difference between air and water [Cortinovis and Song, 2005].

There are some factors that directly influence the efficiency of the cooling tower. The wet bulb temperature has a great influence on the tower design, being therefore of great influence in the operation of the tower. With the high variation of the wet bulb temperature relative to the design reference temperature, the plant's operating efficiency is reduced. Other factors that influence the performance of cooling towers are the range, approach, the volumetric flow of water and the evaluation factor.

Modeling involves heat and mass transfer phenomena of both air and water streams, with complex interactions. Accurate analytical or numerical modeling aims to reproduce wet

cooling tower behavior with different accuracy levels. However, some operation issues, like decreasing capacity, leakages, and environmental changes, are not easily modeled. Several studies emphasized these limitations, thus justifying the use of models based on Artificial Neural Networks ANN [Cortinovis et al., 2009a; Jasiulionis, 2012; Qi et al., 2016; Wu et al., 2018].

This work aims to evaluate the capacity of an Artificial Neural Network ANN developed for a reference cooling tower to reproduce the behavior of similar equipment. This ANN can be seen as a research tool for problem identification, as it can compare operational data from a given tower to a reference case.

4.2 Problem description

PECEM site hosts two independent 360 MW subcritical coal-fired power plants, with identical design, here referred to as GP1 and GP2. Heat rejection is performed by a set of 16 wet cooling towers per plant, as a part of the condensation circuit connected to the plant, presented in Figure 4.2 (a). Figure 4.2 (b) shows a schematic view of the water and air counter flows of one cooling tower unit with its main operational mass flow parameters.

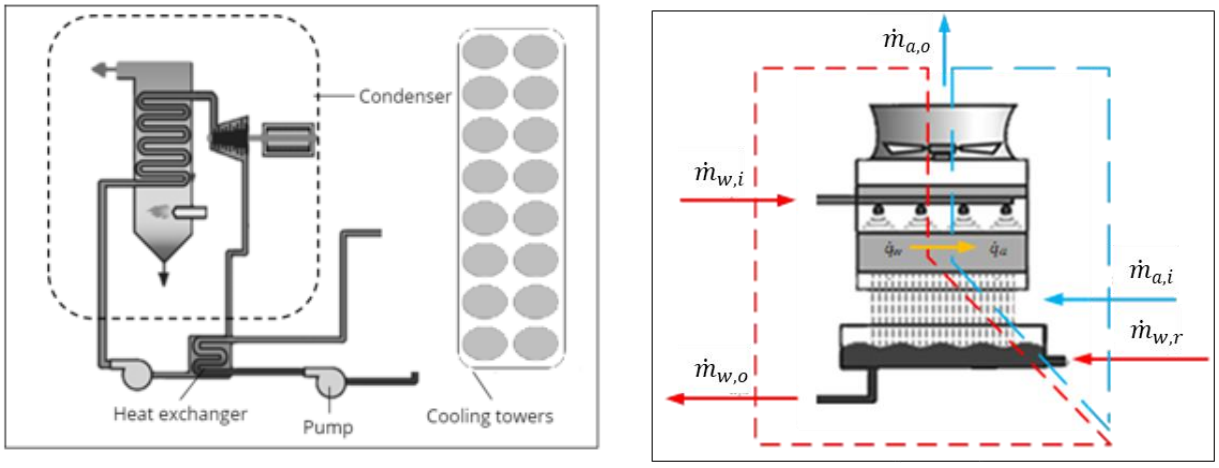

(a) **(b)**

Figure 4.2 - (a) PECEM plant cooling system composed by the condenser heat exchanger, pump and cooling tower assembly, (b) Schematic representation of a cooling tower.

Hot water from the condenser is admitted into the tower at a mass flow rate of $\dot{m}_{w,i}$ releases heat to the air $\dot{q}_w$ and returns to the plant condenser at a mass flow rate of $\dot{m}_{w,o}$. Makeup water at mass flow rate of $\dot{m}_{w,r}$ is added to compensate water evaporation and drag

to the atmosphere, which is accounted to the output air mass flow rate $\dot{m}_{air,o}$ in the present mass balance.

Table 4.1 presents some common operational parameters for each of the plants, designed to deliver a gross 360 MW electric power output, 1134 t/h of superheated steam at 180 bar and 541 ºC and steam backpressure of 85 mbar.

Table 4.1 - Operating range of the two towers parameters

Parameter	Abbreviation	Minimum	Maximum
Power generation	P	200.27 MW	363.52 MW
Vapor back pressure	BP	67.57 mbar	1038.36 mbar
Air dry bulb temperature	T_{db}	18.73 ºC	36.55 ºC
Air wet bulb temperature	T_{wb}	17.71 ºC	27.86 ºC
Tower water output temperature	T_{out}	27.70 ºC	38.02 ºC
Tower water input temperature	T_{in}	37.87 ºC	54.38 ºC

T_{db} and T_{wb} are useful parameters to model cooling tower operation as the last one is determinant to the plant efficiency. However, the nearest weather station was located 50 kilometers far from PECEM, and do not represent the plant site conditions. Makeup water mass flow is another key parameter for tower modeling, but its flow was only accounted on monthly basis. Heat rejection $\dot{Q}_{rej}$from the tower to the environment was then estimated with the aid of available parameters, as shown in Equation 4.1.

$$\dot{Q_{rej}} = \dot{m}_{w,t}\, cp_w\, \Delta T_w \tag{4.1}$$

where $\dot{m}_{w,t}$ is the tower water flow, where $\dot{m}_{w,t} = \dot{m}_{w,i} = \dot{m}_{w,o}$, cp_w is the water specific heat and ΔT_w the temperature difference $\Delta T_w = T_{out} - T_{in}$. The makeup water mass flow rate $\dot{m}_{w,r}$ was estimated based on Equation 4.2.

$$\dot{m}_{w,r} = \frac{\dot{Q_{rej}}}{i_{l,v}\, \rho} \tag{4.2}$$

with $i_{l,v}$ is the water latent heat of vaporization and ρ is the water liquid phase density.

Although sharing the same design, plants actually display slightly different operating conditions and performances, resulting in different vapor backpressure values. Plant operator indicated GP1 to be the reference case due to its reliability and better performance.

4.3 Methodology

A two-step methodology is presented to identify equipment operational problems or deviations in respect to a reference basis. Operational parameters such as Power generation *P*, vapor back pressure *B*P, tower water output and input temperatures T_{out} and T_{in} were acquired from the plant supervisory system and organized together with the calculated rejected heat $\dot{Q}_{rej}$, Equation 4.1, and the makeup water mass flow rate $\dot{m}_{w,r}$, Equation 4.2, to compose two separate dataset for GP1 and GP2 cooling towers. Firstly, a statistic assessment was performed for two the cooling tower datasets, followed by the ANN development to estimate makeup water mass flow rate and heat rejection.

4.3.1 Statistical analysis

Operational parameters were acquired from the plant supervisory system in respect to the electric output range from 240 MW to 360 MW, with additional filtering to exclude invalid data such as zeros and negative values, which referred to the plant shutdowns or measurement errors. Datasets were processes with Minitab, Figure 4.3 and Table 4.2 show the correlation matrix and the Pearson correlation index for GP1.

Table 4.2- Dataset Pearson correlation index for GP1

	P	BP	T_{in}	T_{out}	$\dot{m}_{w,r}$	$\dot{Q}_{rej}$
P	1					
BP	-0.70	1				
T_{in}	0.61	0.95	1			
T_{out}	0.09	0.59	0.67	1		
$\dot{m}_{w,r}$	0.94	0.84	0.80	0.19	1	
$\dot{Q}_{rej}$	0.74	0.89	0.90	0.28	0.92	1

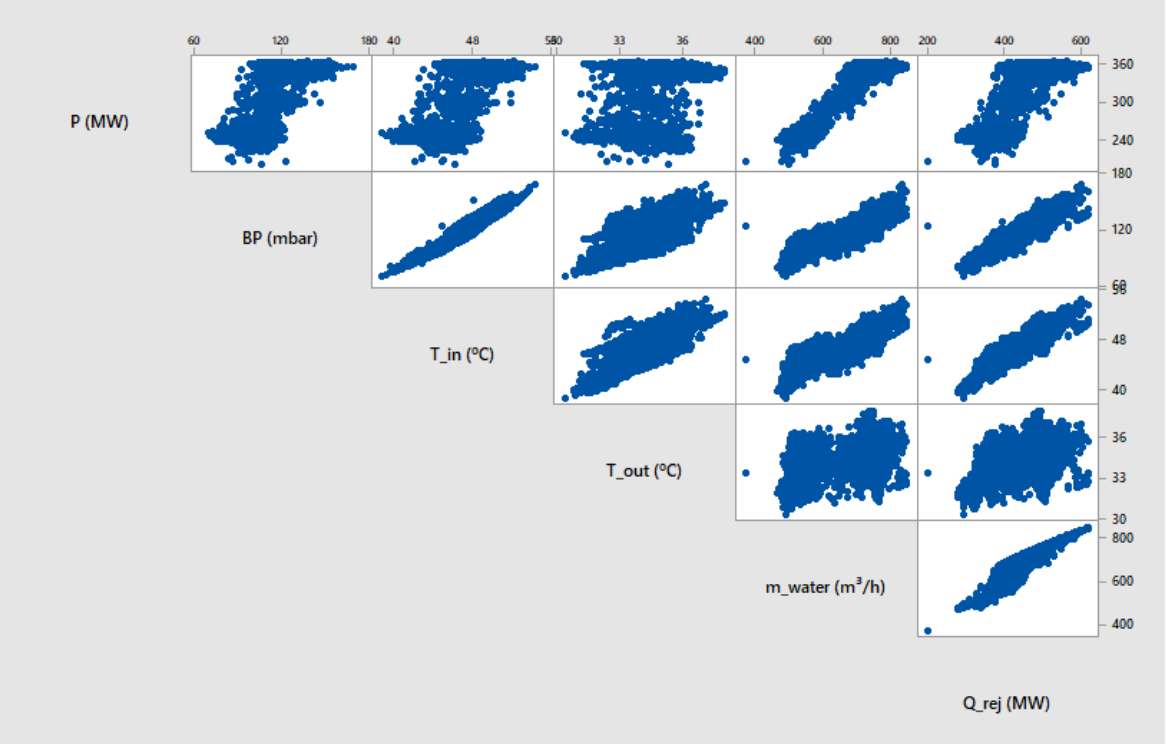

Figure 4.3 - Matrix correlation for GP1.

Heat rejected $\dot{Q}_{rej}$ presented high correlation with vapor backpressure *BP* and water input temperature T_{in}, with Pearson index close to 1. Makeup water flow rate $\dot{m}_{w,r}$ presented high correlation with power generation *P*, vapor backpressure *BP* and water input temperature T_{in}. Low Person correlation indexes were found for water output temperature T_{out} for the two calculated parameters $\dot{m}_{w,r}$ and $\dot{Q}_{rej}$. Figure 4.4 and Table 4.3 presents a similar assessment applied to GP2.

Table 4.3- Dataset Pearson correlation index for GP2

	P	BP	T_{in}	T_{out}	$\dot{m}_{w,r}$	$\dot{Q}_{rej}$
P	1					
BP	0.76	1				
T_{in}	0.72	0.94	1			
T_{out}	0.32	0.46	0.53	1		
$\dot{m}_{w,r}$	0.89	0.82	0.78	0.13	1	
$\dot{Q}_{rej}$	0.61	0.72	0.69	-0.07	0.90	1

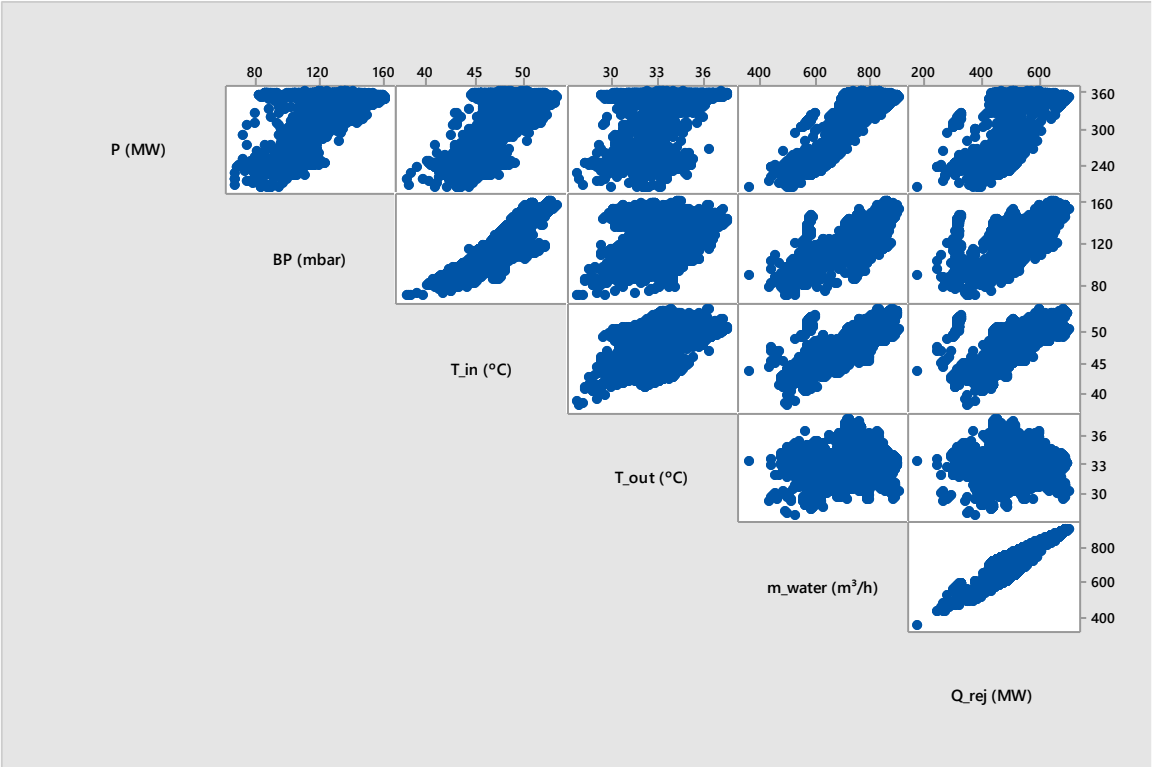

Figure 4.4 - Matrix correlation for GP2.

Results for the Person correlation index in respect to GP2 showed similar trends when compared to GP1, but with different intensities and even slope inversions. That observation allows to induce that the two generating plants operate under particular conditions.

Figure 4.5 brings plots of the rejected heat in respect to the measured parameters for GP1 (left side column) and GP2 (right side column).

Figure 4.6 brings the same organization proposed in Figure 4.5 for the makeup water mass flow rate $\dot{m}_{w,r}$ with respect to the measured parameters for GP1 (left side column) and GP2 (right side column).

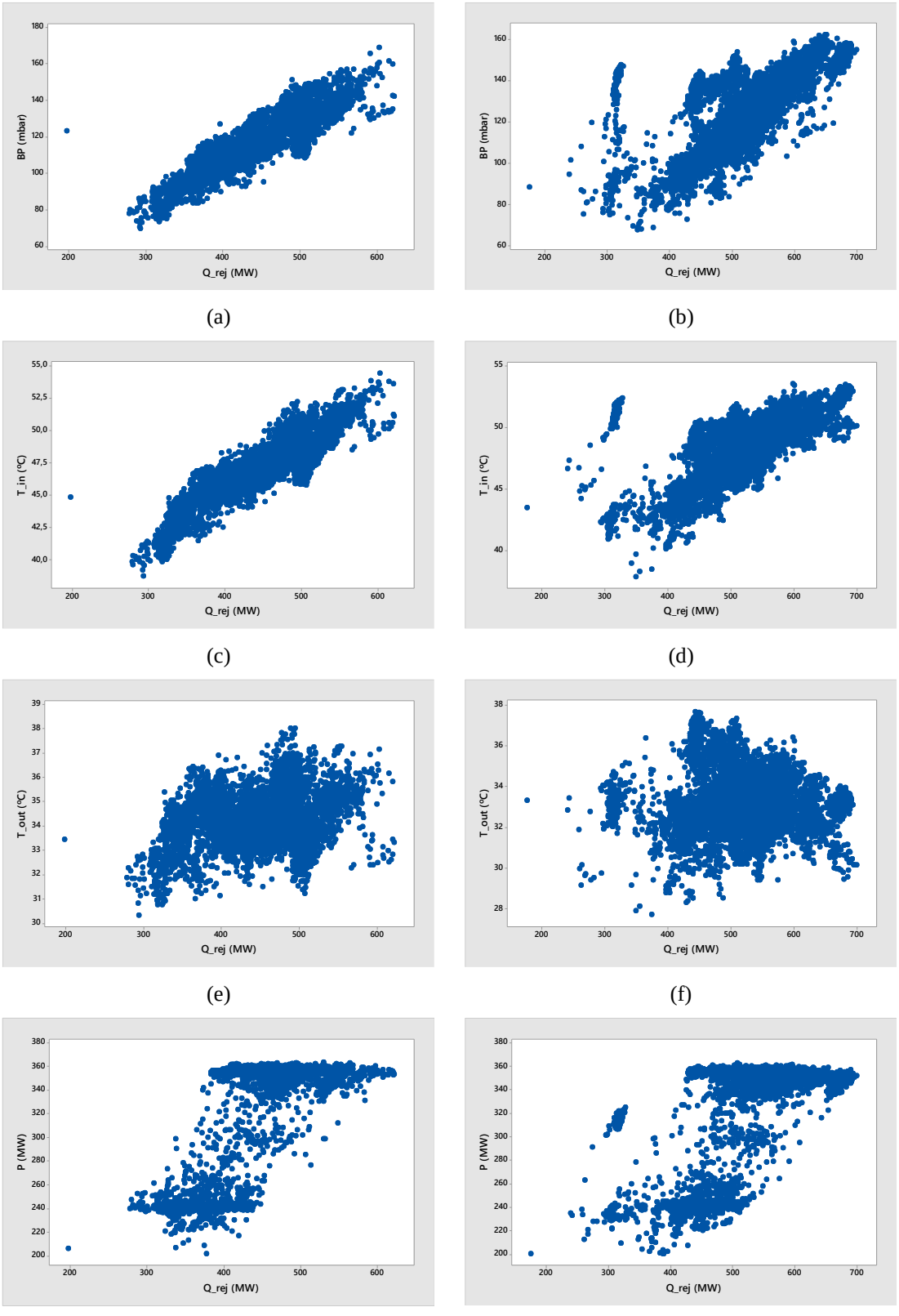

Figure 4.5 - Data plotting with the behavior of the rejected heat $\dot{Q}_{rej}$ respect to the measured parameters vapor backpressure *BP*, input and output water temperature T_{in} and T_{out} and power generation *P* for GP1 (a to d) and GP2 (e to h).

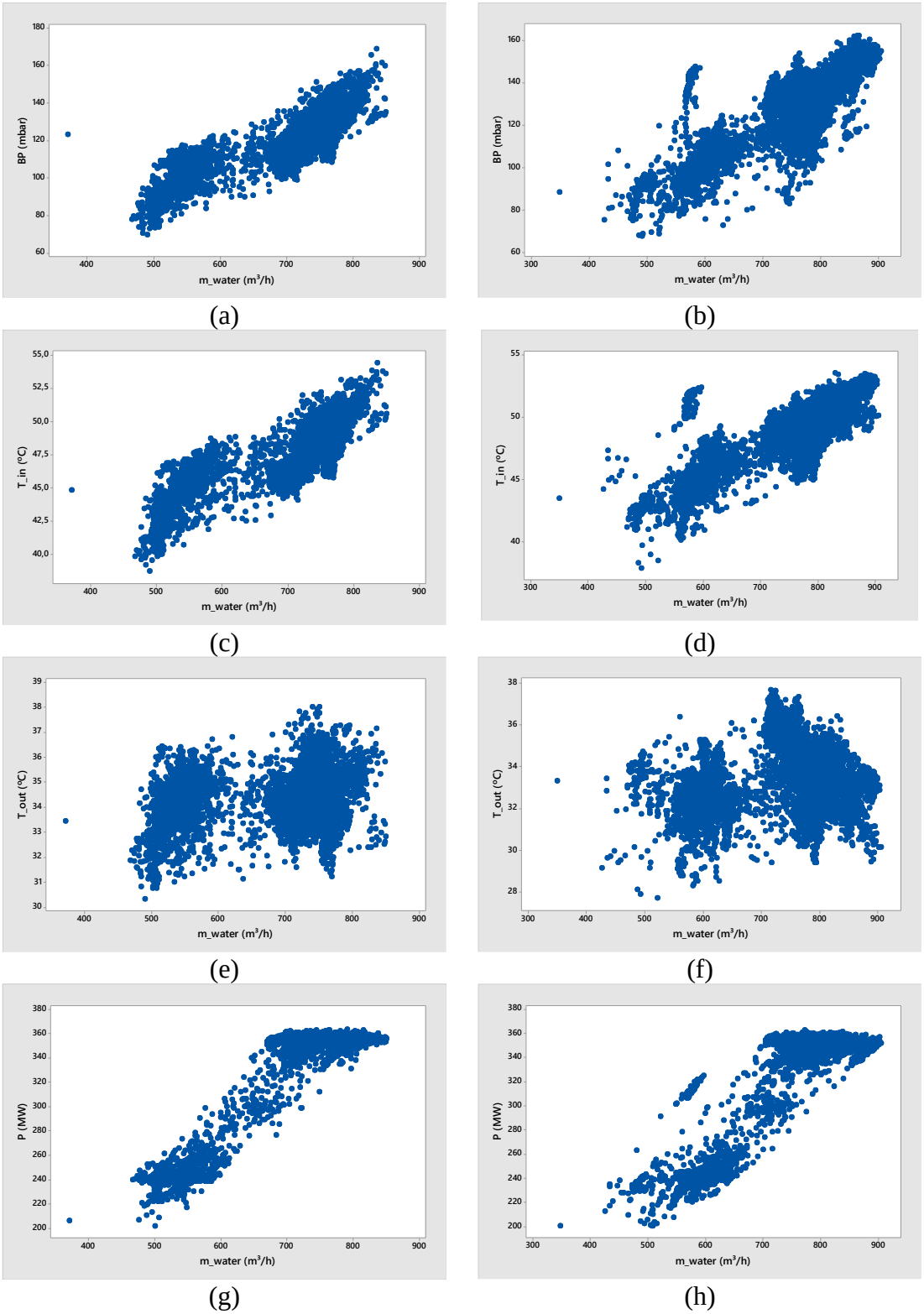

Figure 4.6 - Data plotting with the behavior of the makeup water mass flow rate $\dot{m}_{w,r}$ in respect to the measured parameters vapor backpressure *BP*, input and output water temperature T_{in} and T_{out} and power generation *P* for GP1 (a to d) and GP2 (e to h).

It is possible to identify that GP1 and GP2 presented similar behavior, but with different intensities. Backpressure BP presented a direct relation to rejected heat with less dispersion for GP1 when compared to GP2 (plots *a* and *e*). Some outline data could be identified on plot *e* around the main concentration of measured points, and the same observation can be extended to the remaining plots. Power generation *P* versus rejected heat $\dot{Q}_{rej}$ (plots *d* and *h*) allows to identify two operational baselines, one around 360 MW and another around 240 MW, with the intermediate points probably referring to power range changes.

The same trends formerly presented in respect to the rejected heat in Figure 4.5 can be observed for the makeup water mass flow rate in Figure 4.6. These findings suggest that there are differences concerning the power plants that justify the evaluation of the role of their cooling towers.

4.3.2 Artificial neural network

The ANN models were built based on the GP1 dataset after the examination of the independency and cross correlation of the input parameters. Model performance was assessed by the mean absolute error MSE (4.3), the root mean squared error RMSE (4.4), the mean absolute error MAE (4.5), and the coefficient of determination R^2 (4.6), presented in Equations (4.3) to (4.6).

$$MSE = \left(\frac{1}{n}\sum_{i=1}^{n}(X_{est} - X_{obs})^2\right) \tag{4.3}$$

$$RMSE = \sqrt{\frac{1}{n}\sum_{i=1}^{n}(X_{est} - X_{obs})^2} \tag{4.4}$$

$$MAE = \left(\frac{1}{n}\sum_{i=1}^{n}|X_{est} - X_{obs}|\right) \tag{4.5}$$

$$R^2 = \left(1 - \frac{\sum_{i=1}^{n}(X_{obs} - X_{est})^2}{\sum_{i=1}^{n}(X_{obs})}\right) \tag{4.6}$$

with *X* the steam mass flow rate for both measured (obs) and estimated (est) values and *n* the number of data points.

Two separate ANN models were developed to estimate rejected heat and the makeup water mass flow rate, with a common set of four input parameters, as presented in Figure 4.7.

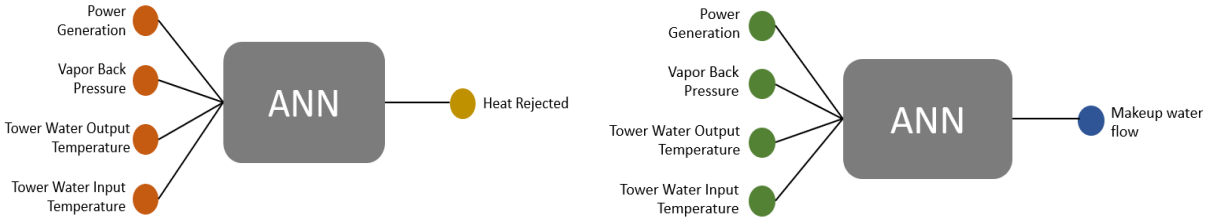

(a) (b)

Figure 4.7 – ANN inputs (a) heat rejected and (b) makeup water mass flow rate.

Models were built following a two-stage procedure. The first one consisted on the ANN training based on GP1 dataset, and comprehended the definition of the number of hidden layers and neurons. The resulting network was a feed forward perceptron multilayer structure, with back propagation mechanism. A sigmoidal hyperbolic tangent function (tansig) was selected as transition function. Dataset was normalized for the -1 to +1 range to be further on divided in 70% for training, 15% for testing and 15% for validation. Matlab was used to build the ANN models, whose details and configurations are presented in the next section. The second stage of the methodology was dedicated to identify operational deviations of GP2 in respect to the reference case by feeding the GP1 ANN with data from GP2.

4.4 Results and discussion

ANN accuracy was assessed by searching the combination of number of neurons and hidden layers capable of achieving low MSE values (4.3) in respect to the observed data. Four ANN models were proposed to simulate the rejected heat rate $\dot{Q}_{rej}$ and the makeup water mass flow rate $\dot{m}_{w,r}$ separately with data from the GP1 dataset. Results reported in Table 4.4 were ranked in respect to the rejected heat rate mean absolute error MSE. The first number after the label ANN indicates the model number of inputs. Each case is reserved to a given hidden layer and the digit indicates the number of neurons per hidden layer.

Table 4.4- ANN configuration analysis GP1

ANN configuration	Makeup water mass flow rate MSE (%)	Heat rejected MSE (%)
ANN_4_4_4_1	0.0013	0.0032
ANN_4_8_8_1	0.033	0.076
ANN_4_4_4_4_1	0.0056	0.0058
ANN_4_16_16_1	0.033	0.0052

The smallest MSE was found for the first ANN model, with 4 inputs, 3 hidden layers with 4 + 4 +1 neurons per layer, respectively, for both $\dot{Q}_{rej}$ and $\dot{m}_{w,r}$. That same ANN model was tested with the GP2 dataset and results are shown in figures 4.8 and 4.9.

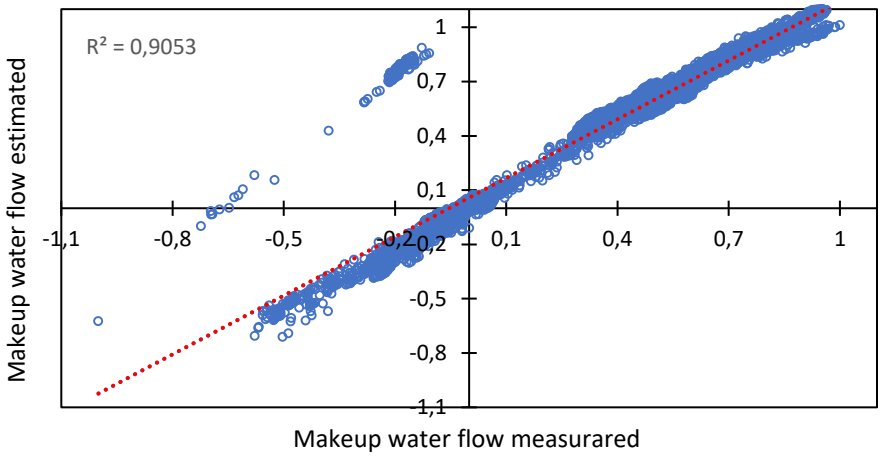

Figure 4.8 – Estimated *vs.* calculated results for the normalized makeup water mass flow rate with ANN_4_4_4_1 (Table 4.4) for GP2 dataset.

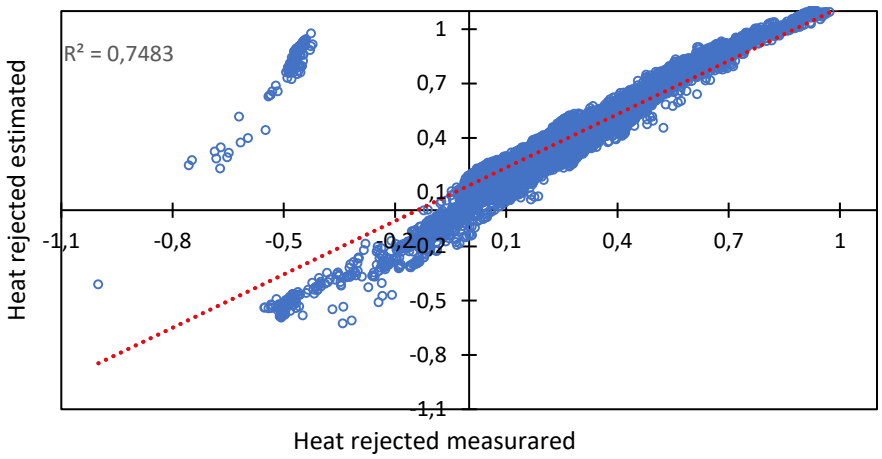

Figure 4.9 - Estimated *vs.* calculated results for the normalized heat rejected rate with ANN_4_4_4_1 (Table 4.4) for GP2 dataset.

The ANN_4_4_4_1 model built with the GP1 dataset proved to be able to estimate both $\dot{Q}_{rej}$ and $\dot{m}_{w,r}$ values from the GP2 dataset with R² of 0.7483 and 0.9053. Some outliers were not captured by the ANN, like the ones already observed in plots *e* to *h* in figures 4.5 and 4.6, which are off standard operational points. That apparent lack of accuracy can be actually used as a tool to identify anomalous or off standard operational points. These former points were removed from GP2 dataset in order to evaluate the performance of the ANN models in estimating the output parameters, as shown in figures 4.10 and 4.11, expressed on the original operational units.

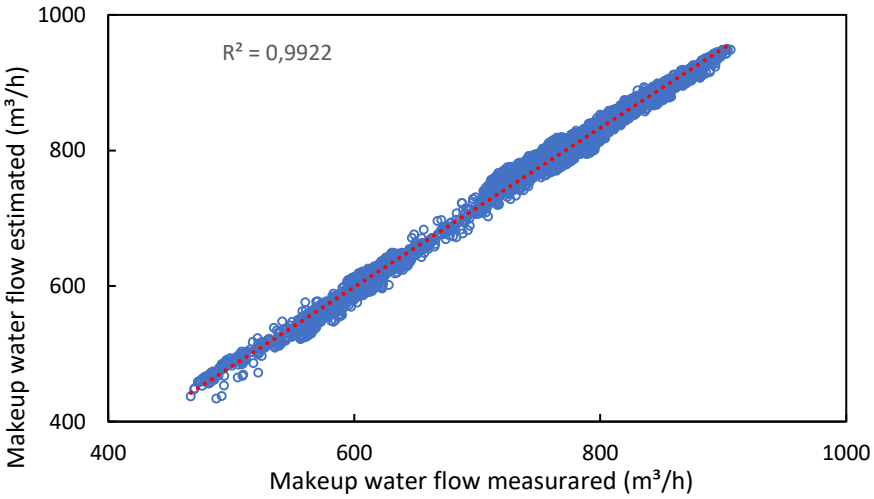

Figure 4.10 – Estimated *vs.* calculated results for the makeup water mass flow rate with ANN_4_4_4_1 (Table 4.4) for GP2 dataset.

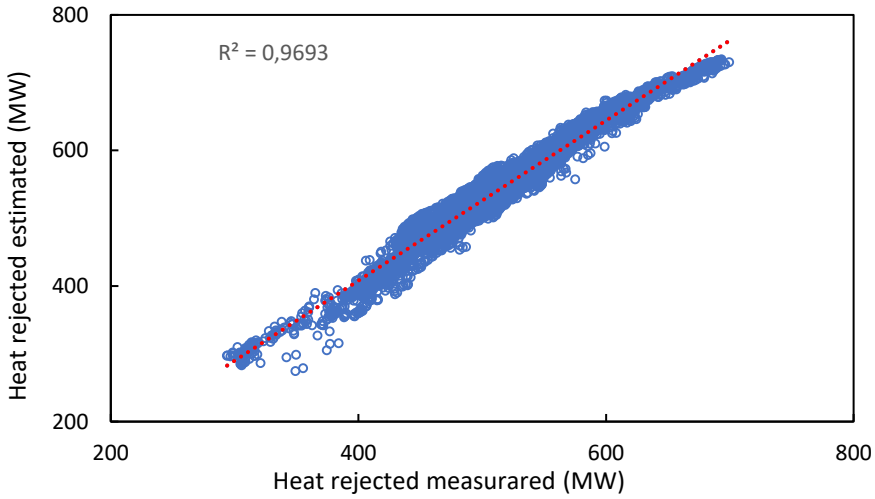

Figure 4.11 - Estimated *vs.* calculated results for the heat rejected rate with ANN_4_4_4_1 (Table 4.4) for GP2 dataset.

Estimation accuracy increased from R^2 values of 0.7483 and 0.9053 to 0.9693 and 0.9922 for $\dot{Q}_{rej}$ with MAE value of 31.37 MW and 35.58 MW of RMSE. For $\dot{m}_{w,r}$ the MAE value is equal to 26.09 m³/h and RMSE value of 29.55 m³/h. It is worth mentioning that the rejected heat rate can range from 290 to 700 MW and the makeup water mass flow rate from 470 to 900 m³/h, which means that the MAE values present a relative deviation from 4.5% to 10.8% for the heat rejection and from 3.7% to 5.5% for the makeup water mass flow rate. The RMSE values stand for a relative deviation from 5.1% to 12.3% for the first case and from 3.3% to 6.3% for the second one.

The present research looked at some other issues. The water temperature difference established by the cooling tower input and output streams was tested in order to build the equipment ANN, but results have shown that the use of individual parameters instead showed to be more accurate. The rejected heat was also calculated by means of the steam condensation right after the turbine discharge, but it also turned out to be less accurate then the use of separate water tower streams.

4.5 Conclusion

Cooling towers modeling is a complex task and ANN showed to be an adequate and convenient tool to simulate their operational parameters.

This work aimed at developing ANN models based on data from a reference cooling tower and use them to simulate similar towers with different datasets willing to identify equipment operating deviations. In the present work, the dataset from a power plant whose operation was considered as well behaved and stable, called GP1, was taken as a reference to build ANN models to simulate a second tower dataset, GP2, as a tool for identifying malfunctioning or anomalous situations.

It is worth stressing the need to evaluate the ANN architectures for each set configuration, which depends on the complexity of the problem. Four parameters were selected as independent input, enabling to calculate the tower rejected heat rate in MW and the makeup water mass flow rate in m³/h.

The best ANN architecture for both calculated outputs was found with three hidden layers, with four neurons on the first and second ones, and one neuron on the last one, with mean absolute error MSE of 0.0032% and 0.0013% for the rejected heat rate and the makeup water mass flow rate respectively.

ANN models built with GP1 data were tested with the GP2 dataset, and the coefficient of correlation R^2 was found to be 0.748 and 0.905 for the rejected heat rate and the makeup water mass flow rate. Although less accurate, that result helped to identify some non-standard behavior of the tower. Therefore, another simulation was performed with a new set of operational data without the GP2 outlier points to give R^2 values of 0.98 and 0.99. Finally, it is worth mentioning that the ANN models were able to identify outliers on the tower rejected heat rate and the makeup water mass flow rate from reliable datasets.

5 CONCLUSIONS

The aim of the present study was to develop models capable of reproducing the PECEM coal-fired power plant equipment. ANN models were used to estimate the steam flow of the PECEM power plant, the rejected heat and the make-up water flow of the PECEM power plant cooling tower. In the second chapter, several studies were presented with ANN models of power plants and related process. They pointed out the satisfactory performance of this methodology in complex problems, such as coal-fired power plants and related processes.

The ANN developed for the steam mass flow rate of the power plant was presented in Chapter 3. In this study, two models were developed, linear multivariable regression and an ANN model. The study evaluated the training group size, the number of inputs and the operation stages (240MW, 360 MW and transition stage). The best ANN architecture for the eight-input was composed by two hidden layers with sixteen and one neuron (ANN_8_16_1) for 240 MW and three hidden layers with sixteen neurons in the first two layers and one neuron in the last neuron (ANN_8_16_16_1) for 360 MW. For the analysis with three-inputs, the best-performing ANN was with four intermediate layers, six neurons in the first three layers and one in the last (ANN_3_6_6_6_1) for 240 MW and four hidden layers with six in the first three and one in the last one (ANN_3_6_6_6_1) for 360 MW.

In all evaluated cases, ANN models presented lower RMSE values than regressions models. Higher errors were found for the 360 MW power operational stage. Best results were found for the complete dataset analysis. Power operation stage of 360 MW error was approximately 15%, for 240 MW stage was 10%, and 5% for the transition regime. The complete dataset RMSE was less than 3%.

Finally, the best model was compared to the regression model to evaluate the steam generator operation. As an example, when the steam mass flow rate is 1093.4 t/h, the regression model and the ANN model estimate values of 1114.0 t/h and 1088.2 t/h, respectively, resulting in a deviation of 20.6 t/h and 5.16 t/h.

In Chapter 4, an ANN model for a cooling tower was developed. The ANN was developed based on data from a reference (GP1) cooling tower and the model was applied to a similar tower with different datasets (GP2). This application will allow the identification of operational deviations in the equipment. The ANN architectures were also evaluated for each set configuration. Four parameters were selected as independent input, enabling to calculate the tower rejected heat rate in MW and the makeup water mass flow rate in m^3/h. For both models, the ANN architecture with higher performance was found with three hidden layers,

with four neurons on the first and second ones, and one neuron on the last layers (ANN_4_4_4_4_1), with MSE values of 0.0032% and 0.0013% for the rejected heat rate and the makeup water mass flow rate respectively.

The ANN models built with GP1 data were tested in the GP2 dataset to evaluate the model capacity in reproducing the cooling tower operation of similar equipment. In this analysis, the coefficient of correlation was found equal to 0.748 and 0.905 for the rejected heat rate and the makeup water mass flow rate respectively. This analysis result helped to identify outlier behavior points of the equipment. Removing the non-standard points from the dataset, the model gives R^2 values of 0.98 for the rejected heat rate and 0.99 for the makeup water mass flow rate. To conclude, the analysis developed in this chapter allows concluding that the ANN models were able to identify non-standard points on the cooling tower.

5.1 Future works

Future work could be the evaluation of variables with statics analysis and the development of models for other important equipment and processes based on PECEM plant dataset. As such, models can be associated to simulate the complete process of the power plant, and to promote their coupling to the supervisory control and data acquisition system in order to assist the operator in the decision-making process.

In addition, the models developed in this work could be applied to the same equipment but in different environments. The application of these models will facilitate the modeling of the equipment, allowing a focus on process improvement studies.

6 PUBLICATIONS

Helena Reichert, Paulo Schneider, João Fonseca. STEAM FLOW ESTIMATION WITH ARTIFICIAL NEURAL NETWORK BASED ON POWER PLNAT OPERATION DATA. ENCIT 2018.

Helena Reichert, Bruno Schneider, Paulo Schneider, Guilherme Oliveira. PERFORMANCE ESTIMATION OF A COOLING TOWER USING NA ANN MODE. ECOS 2019.

BIBLIOGRAPHY

Abbassi, A. and Bahar, L. Application of neural network for the modeling and control of evaporative condenser cooling load, **Applied Thermal Engineering**, vol. 25 (17-18), p. 3176-3186, 2005.

ANEEL. **BIG - Banco de Informações de Geração**. http://www2.aneel.gov.br/aplicacoes/capacidadebrasil/capacidadebrasil.cfm, 2018, Accessed 27-07-2018.

ASHRAE. **ASHRAE handbook: heating, ventilating, and airconditioning systems and equipment**, SI Edition, 2016.

Bazzo, E. **Geração de vapor**. Florianópolis: Editora da Universidade Federal de Santa Catarina, 1995.

Bekat, T., Muharrem, E., Fikret, I. and Ayten, G. Prediction of the bottom ash formed in a coal-fired power plant using artificial neural networks, **Energy**, vol. 45 (1), p. 882–887, 2012.

Cooling Tower Institute. Houston. **Apresenta recursos e atividades desenvolvidas**. http://www.cti.org, 2019, Accessed 20-01-2019.

Cortinovis, G. F. Paiva, J. L., Song, T. W. and Pinto, J. M. A systemic approach for optimal cooling tower operation, **Energy Conversion and Management**, vol. 50 (9), p. 2200–2209, 2009 (a).

Cortinovis, Giorgia F. Ribeiro, M. T., Paiva, J. L., Song, T. W. and Pinto, J. M. Integrated analysis of cooling water systems: Modeling and experimental validation, **Applied Thermal Engineering,** vol. 29 (14–15), p. 3124–3131, 2009 (b).

Cortinovis, G. F. and Song, T. W. **Funcionamento de uma Torre de Resfriamento de Água**. São Paulo, 2005.

Dave, V. S. and Dutta, K. Neural network based models for software effort estimation: A review, **Artificial Intelligence Review**, vol. 42 (2), p. 296-307, 2014.

De, S., Kaiadi, M. Fast, M. and Assadi, M. Development of an artificial neural network model for the steam process of a coal biomass cofired combined heat and power (CHP) plant in Sweden, **Energy**, vol. 32 (11), p. 2099–2109, 2007.

Deshpande, P., Warke, N., Khandare, P. and Deshpande, V. Thermal Power Plant Analysis Using Artificial Neural Network, **3rd Nirma University International Conference on Engineering**, p. 6–8, 2012.

Estiati, I., Freire, F. B., Freire, J. T., Aguado, R. and Olazar, M. Fitting performance of artificial neural networks and empirical correlations to estimate higher heating values of biomass, **Fuel**, vol. 180, p. 377–383, 2016.

European Environment Agency. **Global and European sea level**, 2017.

Fan, H., Zhang, Y., Su, Z. and Wang, B. A dynamic mathematical model of an ultra-supercritical coal fired once-through boiler-turbine unit, **Applied Energy**, vol. 189, p. 654–666, 2017.

Fast, M. and Palmé, T. Application of artificial neural networks to the condition monitoring and diagnosis of a combined heat and power plant, **Energy**, vol. 35 (2) p. 1114–1120, 2010.

Gevrey, M., Dimopoulos, I. and Lek, S. Review and comparison of methods to study the contribution of variables in artificial neural network models, **Ecological Modelling**, vol. 160 (3), p. 249–264, 2003.

Ghugare, S. B., Tiwary, S., Elangovan, V. and Tambe, S. S. Prediction of Higher Heating Value of Solid Biomass Fuels Using Artificial Intelligence Formalisms, **Bioenergy Research**, vol. 7 (2), p. 681–692, 2014.

Gao, M., Shi, Y. T., Wang, N. N., Zhao, Y. Bin and Sun, F. Z. Artificial neural network model research on effects of cross-wind to performance parameters of wet cooling tower based on level Froude number, **Applied Thermal Engineering**, vol. 51(1–2), p.1226–1234, 2013.

Han, J., Kamber, M. and Pei, J. **Data Mining: Concepts and Techniques**. Morgan Kaufmann, San Francisco, 3 edition, 2012.

Haykin, S. **Redes neurais: princípios e prática.** Bookman, São Paulo, 2 edition, 2001.

Haykin, S. **Neural Networks and Learning Machines**. Pearson, New Jersey, 2 edition, 2009.

Hübel, M., Meinke, S., André, M. T., Wedding, C. and Nocke, J. Modelling and simulation of a coal-fired power plant for start-up optimization, **Applied Energy**, vol. 208, p. 319–331, 2017.

Hosoz, M., Ertunc, H. M. and Bulgurcu, H. Performance prediction of a cooling tower using artificial neural network, **Energy Conversion and Management**, vol. 48, p. 1349-1359, 2007.

International Energy Agency. **Key world energy statistics**, 2017.

Jasiulionis, J. A. E. Design and analysis of cooling towers using neural networks. 2012. Universidade Estadual de Campinas Faculdade, 2012.

Kavzoglu, T. Determining Optimum Structure for Artificial Neural Networks, **Proceeding of the 25th Annual Technical Conference and Exhibition of the Remote Sensing Society**, n. September, p. 675–682, 1999.

Kopanos, G. M., Murele, O. C., Silvente, J., Zhakiyev, N., Akhmetbekov, Y. and Tutkushev, D. Efficient planning of energy production and maintenance of large-scale combined heat and power plants, **Energy Conversion and Management**, vol. 169, p. 390–403, 2018.

Lecun, Y., Bengio, Y. and Hinton, G. Deep learning, **Nature**, vol. 521 (7553), p. 436-444, 2015.

Li, J., Ososanya, E.T. and Smoak, R.A. The neural network control application in a power plant boiler, **Institute of Electrical and Electronics Engineers (IEEE)**, p. 521-524, 2002.

Liu, J. Z., Yan, S., Zeng, D. L., Hu, Y. and Lv, Y. A dynamic model used for controller design of a coal fired once-through boiler-turbine unit, **Energy**, vol. 93, p. 2069–2078, 2015.

Mahdi, Q. S., Saleh, S. M. and Khalaf, B. S. Investigation of natural draft cooling tower

performance using neural network, **In Springer Proceedings in Physics**, vol. 155, p. 315–327, 2014.

Mendel, J. M. and McLaren, R. W. Reinforcement-learning control and pattern recognition systems, **Mathematics in Science and Engineering**, vol. 66 (C), p. 287-318, 1970.

Mesroghli, S., Jorjani, E. and Chehreh ChelganI, S. Estimation of gross calorific value based on coal analysis using regression and artificial neural networks, **International Journal of Coal Geology**, vol. 79(1-2), p. 49–54, 2009.

Mohanraj, M., Jayaraj, S. and Muraleedharan, C. Applications of artificial neural networks for thermal analysis of heat exchangers - A review, **International Journal of Thermal Sciences**, vol. 90, p. 150-172, 2015.

Nowak, G. and Rusin, A. Using the artificial neural network to control the steam turbine heating process, **Applied Thermal Engineering**, vol. 108, p. 204–210, 2016.

Oko, E., Wang, M. and Zhang, J. Neural network approach for predicting drum pressure and level in coal-fired subcritical power plant, **Fuel**, vol. 151, p. 139–145, 2015.

Qasim, S. M. and Hayder, M. J. Parametric study of closed wet cooling tower thermal performance. **IOP Conference Series: Materials Science and Engineering**, 227(1), 2017.

Qi, X., Liu, Y., Guo, Q., Yu, S. and Yu, J. Performance prediction of a shower cooling tower using wavelet neural network, **Applied Thermal Engineering**, vol. 108, p. 475–485, 2016.

Rojas, R. Neural Networks: A Systemic Introduction, **Neural Networks**, vol. 7 (1), p. 509, 1996.

Silva Neto, A. and Becceneri, J. C. **Técnicas de inteligência computacional inspiradas na natureza: aplicação em problemas inversos em transferência radiativa.** SBMAC, São Carlos, 2009.

Smrekar, J., Assadi, M., Fast, M., Kuštrin, I. and De, S. Development of artificial neural network model for a coal-fired boiler using real plant data, **Energy**, vol. 34 (2), p. 144–152, 2009.

Starkloff, R., Alobaid, F., Karl, K., Eppel, Bernd. and Schmitz, M. Development and validation of a dynamic simulation model for a large coal-fired power plant, **Applied Thermal Engineering**, vol. 91, p. 496–506, 2015.

Strušnik, D. and Avsec, J. Artificial neural networking and fuzzy logic exergy controlling model of combined heat and power system in thermal power plant, **Energy**, vol. 80, p. 318–330, 2015.

Strušnik, D., Golob, M. and Avsec, J. Artificial neural networking model for the prediction of high efficiency boiler steam generation and distribution, **Simulation Modelling Practice and Theory**, vol. 57, p. 58–70, 2015.

Suresh, M. V. J. J., Reddy, K. S. and Kolar, A. K. ANN-GA based optimization of a high ash coal-fired supercritical power plant, **Applied Energy**, vol. 88, n. 12, p. 4867–4873, 2011.

Torreira, R. P. **Geradores de vapor**. São Paulo: Companhia Melhoramentos. 1995.

Tunckaya, Y. and Koklukaya, E. Comparative prediction analysis of 600 MWe coal-fired power plant production rate using statistical and neural-based models, **Journal of the Energy Institute**, vol. 88 (1), p. 11–18, 2015(a).

Tunckaya, Y. and Koklukaya, E. Comparative analysis and prediction study for effluent gas emissions in a coal-fired thermal power plant using artificial intelligence and statistical tools, **Journal of the Energy Institute**, vol. 88 (2), p. 118–125, 2015(b).

Wu, J., Cao, L. and Zhang, G. Artificial neural network analysis based on genetic algorithm to predict the performance characteristics of a cross flow cooling tower. **IOP Conference Series: Earth and Environmental Science**, vol. 121 (5), p. 0–9, 2018.

Zhang, C., Wang, Y., Zheng, C., Lou, X. Exergy cost analysis of a coal fired power plant based on structural theory of thermoeconomics, **Energy Conversion and Management**, vol. 47(7–8), p. 817–843, 2006.